Tan H., Seno M., et al	Construction of a high-efficiency multi-site-directed mutagenesis.	African J Biotechnol	10 (3)	449-452	2011
Tan H., Seno M., et al	The conformational polymorphism of the green fluorescent protein.	Molecular Biology	46 (1)	142-148	2012
Katayama S., Futaki S., et al	Acylation of octaarginine: Implication to the use of intracellular delivery vectors.	J Control Release	149	29-35	2011
Akita H., Futaki S., et al	Nanoparticles for ex vivo siRNA delivery to dendritic cells for cancer vaccines: Programmed endosomal escape and dissociation	J Control Release	149	58-64	2011
Nakase I., Futaki S., et al	Efficient intracellular delivery of nuclei acid pharmaceuticals using cell -penetrating peptides.	Acc Chem Res	印刷中		2011
Hirose H., Futaki S., et al	Transient focal membrane deformation induced by arginine-rich peptides leads to their direct penetration into cells.	Mol Ther	印刷中		2012
Nakase I., Futaki S., et al	Accumulation of arginine-rich cell-penetrating peptides in tumors and the potential for anticancer drug delivery in vivo.	J Control Release	印刷中		2012

Ⅳ. 研究成果の刊行物・別刷

Nanoparticle-based Drug Delivery Systems for Solid Brain Tumors

Bin Feng[1,2], Hideki Matsui[2] and Kazuhito Tomizawa[3,*]

[1]*Department of Biotechnology, Dalian Medical University, Dalian 116044, China,* [2]*Department of Physiology, Okayama University Graduate School of Medicine, Dentistry and Pharmaceutical Sciences, Okayama 700-8558, Japan,* [3]*Department of Molecular Physiology, Faculty of Life Sciences, Kumamoto University, Kumamoto 860-8558, Japan*

Abstract: The treatment of brain tumors including glioblastoma multiformes (GBMs) remains a challenge. The main option is still surgery to remove the bulk of the tumor and adjuvant treatments for the infiltrating parts. The blood brain barrier (BBB), however, restricts the access of chemotherapeutic agents to the tumor. The use of nanoparticle-based drug delivery systems (DDSs) has an increasing impact on disease diagnosis and therapy. By altering their size, composition, and surface chemistry, nanoparticles can be developed into a universal platform with multifunctional capabilities to meet the tunable requirements of different DDS. Thus, nanoparticles have the potential for targeted delivery of therapeutic cargo to brain tumors combined with simultaneous detection and imaging functions, providing a new strategy for effective therapy. The purpose of this article is to provide an updated review on the current progression and future possibilities of treating brain tumors with nanoparticles.

Keywords: Nanoparticles, targeted drug delivery, blood-brain barrier, imaging; therapy.

1. INTRODUCTION

Brain tumors are a heterogeneous group of neoplasms, each with its own characteristics, treatment, and prognosis. For most intracranial tumors, the clinical diagnostic approach and initial treatment are similar [1]. Glioblastoma multiforme (GBM) is one of the most malignant and aggressive brain tumors. The local infiltration of high-grade glioblastomas prevents the complete resection of all malignant cells. Although at present, treatment mainly consists of surgery and radiotherapy [2], it is difficult to remove all the cancerous tissues without severely damaging the brain, and healthy brain tissue is less tolerant to conventional radiotherapy than tumor tissue. Moreover, glioblastomas are resistant to radiation. Although surgery together with chemotherapy is generally performed for brain tumors, malignant brain tumors are the most lethal primary tumors because of difficulties with the targeted delivery of anti-tumor drugs [3]. The delivery of drugs to the brain needs a special strategy to bypass the blood brain barrier (BBB). Current drug delivery methods for the brain include: chemical modification of drug and prodrugs; temporary disruption of the BBB; local delivery to the brain; convection-enhanced delivery (CED); and carrier/receptor-medicated delivery [4].

Drug delivery systems (DDS) such as lipid- or polymer-based nanoparticles can be designed to improve the pharmacological and therapeutic properties of drugs administered parenterally [5]. Nanoparticles were first developed three decades ago. Their initial applications were mainly as vaccine carriers and chemotherapeutic agents [6,7]. The use of nanoparticles in DDS will allow practitioners to use drugs to target specific areas of the body. In the treatment of malignancies, the use of nanoparticles as DDS is having a measurable impact. Medical imaging can also utilize DDS to illuminate tumors, the brain, or cellular functions in the body. The utility of nanoparticle-based DDS to improve human health is potentially enormous.

Nanoparticle-based drug delivery has emerged as a potential method for improving the detection and treatment of brain tumors given the non-toxicity and simplicity in surface modifications of nanoparticles [8]. Nanoparticles are stable, solid, colloidal particles consisting of biodegradable polymer or lipid materials and range in size from 10 to 1,000 nm. Desirable properties such as a small size, a high payload, tumor-specific targeting, a long blood circulation time, and the ability to cross the BBB, can be achieved with nanoparticle delivery systems. Moreover, multi-functionality including the detection, treatment and tracking of tumors is another advantage of nanoparticles, leading to informed decisions about further treatment [9]. Nanoparticles can provide many ideal devices for the delivery of specific compounds to brain tumors, loading them into nanoparticle-based carriers *via* a variety of chemical methods including encapsulation, adsorption, and covalent linkage. These nanoparticles are probably internalized into brain tissue, bypassing the BBB, *via* endocytosis by endothelial cells, using different molecularly-based nanoparticle-brain tumor cell interactions.

Nanoparticle research involves the design, synthesis, and characterization of materials and devices that have a functional organization in at least one dimension on a nanometer scale. Advances in nanoparticle research have produced an array of nanoscaled polymeric, liposomal, and inorganic materials as potential drug carriers [10-12]. Using a variety of nanoparticles of different chemical compositions, different groups are exploring proof-of-concept approaches for the delivery of anti-cancer drugs, oligonucleotides, genes, and magnetic resonance imaging (MRI) contrast agents.

Nanoparticles can concentrate in tumor masses, at inflammatory sites, and at infectious sites by virtue of the enhanced permeability and retention (EPR) effect on the vasculature [13]. The EPR effect provides an opportunity for a more selective delivery of nanoparticles (lipid or polymer-conjugated anticancer drugs) to the tumor [14,15]. It is possible for nanoparticles to selectively deliver several different drugs to malignant tissue [16].

The BBB is the most important barrier involved in the regulation of molecules accessing the brain. The BBB is composed of relatively impermeable endothelial cells with tight junctions, enzymatic activity, and active efflux transport systems. The BBB represents an insurmountable obstacle for a large number of drugs, including antibiotics, antineoplastic agents, and a variety of drugs acting on the central nervous system (CNS), especially neuropeptides [17,18]. The opening of tight junctions in cancer cells is one of the most important abnormalities in brain cancer, and becomes more pronounced as the malignancy worsens. However, hyperpermeability occurs mainly in new vessels, whereas barrier function is retained in the growing margins of the tumor [19,20]. The use of nanoparticles to deliver drugs to the brain by infiltrating the BBB

*Address correspondence to this author at the Department of Molecular Physiology, Faculty of Life Sciences, Kumamoto University, Kumamoto 860-8558, Japan: Tel: +81 96 373 5050; fax: +81 96 373 5052;
E-mail address: tomikt@kumamoto-u.ac.jp

1573-4137/11 $58.00+.00

may provide a way to solve this problem. Nanoparticles are excellent tumor-targeting vehicles because of a unique inherent property of solid tumors. Due to their rapid growth, many solid tumors have a fenestrated vasculature and poor lymphatic drainage, resulting in an EPR effect [14], which allows nanoparticles to accumulate specifically at the cancerous site.

Beyond the passive tumor-targeting properties caused by the EPR effect, intratumoral localization of nanoparticles can be further improved by active targeting through the conjugation of the particles with tumor-specific small molecules, such as folic acid [21], thiamine [22], and even antibodies or lectins [23]. The nanoparticles may be special vehicles for the treatment of brain tumors especially primary and metastatic tumors.

2. LIPOSOMES IN DRUG DELIVERY SYSTEMS FOR BRAIN TUMORS

Liposomes, comprised of naturally occurring non-cytotoxic phospholipids and cholesterols, have been recognized as a potential drug delivery vehicle for three decades [24]. Liposomes are unilamellar phospholipid vesicles and their high interior ability to encapsulate water-soluble compounds surpasses that of all other nanomaterial-based drug delivery platforms [25]. Also, by altering lipid composition, size, and surface chemistry, liposomes can be developed into multifunctional constructs to meet the tunable requirements of different DDS, for example, combining diagnostic and therapeutic capabilities, thus providing a universal platform that can simultaneously detect, image, and target diseased cells.

2.1. Immunoliposomes (Antibody-directed Liposomes)

Treatment of brain cancer remains a challenge despite recent improvements in surgery and multimodal adjuvant therapy. Drug therapy has been particularly inefficient, due to the BBB and the non-specificity of the potentially toxic drugs. Immunoliposomes have emerged as a potential carrier for brain delivery, able to overcome the current problems.

In recent years, drug delivery research has increasingly focused on antibody-targeting liposomes in the treatment of cancers including glioblastomas [26]. Targeted liposomes provide an advantage over untargeted liposomes not because of increased localization to tumor sites but because of increased interaction with the target cell population once localized [27]. Immunoliposomes have come to be recognized as a promising tool for the site-specific delivery of drugs and diagnostic agents. It has been demonstrated that the specific delivery of drugs to target cells is far more efficient with immunoliposomes than with liposomes lacking an antibody [27].

In the development of antibody-targeting liposomes, the antibody is first directly conjugated on the liposome surface resulting in immunoliposomes that exhibit specificity in binding but low blood circulation times. Longer blood circulation times of immunoliposomes *in vivo* combined with successful targeting was demonstrated with polyethylene glycol (PEG)-coated liposomes [27]. However, the targeting of immunoliposomes *in vivo* is far more complicated. The rapid uptake of liposomes by the reticuloendothelial system (RES) and the endothelial barriers separating blood and tissues largely prevent immunoliposomes from reaching their target cells [28]. As systemic administration is the most practical route for treatment, immunoliposomes overcoming these physiological barriers are highly desirable. Avoidance of this obstacle is possible if PEG-derivatized lipids are inserted within the bilayer of conventional liposomes and antibodies are attached *via* a thioether bond to the PEG terminus [29-31], as these modifications considerably prolong circulation time in blood. Liposomes coated with the inert and biocompatible polymer PEG are widely used and are commonly called long-circulating or sterically stabilized liposomes. Park *et al.* [32] prepared doxorubicin (dox) encapsulated immunoliposome with anti-HER2, immunoliposome-dox was significantly superior to all other treatment including free dox, liposomal dox, and anti-HER2 monoclonal antibody (mAb). Tumor inhibition, regression, and cures were observed in the tumor xenograft. These long-circulating liposomes have considerable potential as drug carriers for cancer therapy [33,34]. Increased liposome accumulation has been found in tumor-bearing mice.

For the targeted delivery of drugs to brain tumors, the key is to choose an efficient marker on the tumor cells as the target. Epidermal growth factor receptor (EGFR) is a 170-kDa transmembrane tyrosine kinase whose gene is often amplified in human GBMs. EGFRvIII, which has an in-frame deletion of exons 2-7 of the extracellular domain of the EGFR gene, is constitutively expressed and amplified in up to 57% of GMBs [35]. EGFR is overexpressed in GMB, but undetectable or weakly expressed in normal brain cells. Therefore, EGFR is an attractive molecular target for the specific delivery of therapeutic agents to high-grade gliomas [36,37]. An antibody (anti-CD19) can be directly linked to a liposome through covalent conjugation to a functional group on the liposome or can be post-inserted into a preformed liposome *via* the micelles of an antibody–lipid conjugate [38,39]. The efficiency of liposomal and other nanoplatform systems has also been enhanced by the molecular targeting of the interleukin-13 receptor, transferrin receptor, and LDL surface receptor pathways [40].

Doxorubicin and paclitaxel are FDA-approved anticancer drugs that are limited by physiochemical properties that make them difficult to administer or have intolerable side effects. Encapsulated in nanoparticles, modified paclitaxel has an improved side effect profile compared to conventional paclitaxel and the potential life-threatening cardiotoxicity associated with doxorubicin is reduced. Other liposomal anticancer drugs are currently in various stages of development [41]. In a recent *in vivo* murine U87-MG GBM model, liposomal topotecan has been shown to improve overall survival by a factor greater than 20-fold [42].

Although the toxicity of immunoliposomes themselves is generally minimal, immune responses caused by Fc region of murine-derived antibodies and crossreactivity with normal organs are the potential sources of toxicity. Besides, accumulation of cargos in organs including liver, spleen and bone marrow are the major complications of toxicity [27]. Improvement of target specificity or using lower molecular weight targeting moieties such as Fab′ and scFV may solve the problem.

2.2. Immunoliposomes in Boron Neutron Capture Therapy (BNCT) for Brain Tumors

Besides anticancer and chemotherapeutic drug delivery to brain tumors, boron neutron capture therapy (BNCT) provides a way to selectively destroy malignant cells and spare normal cells. BNCT is a binary method for the treatment of cancer based on the tumor-selective delivery of ^{10}B followed by radiation with low energy thermal neutrons. BNCT has been applied clinically to the treatment of malignant brain tumors, malignant melanoma, head and neck cancer, and hepatoma [43]. It is assumed that the selective accumulation of ^{10}B in tumors followed by radiation with low energy thermal neutrons will cause the killing of cancer cells and induce a therapeutic effect [44]. For targeted ^{10}B delivery in BNCT, immunoliposomes have been employed by linking tumor-targeting ligands such as antibodies or receptor ligands such as folate [45], transferrin [46] and epidermal growth factor (EGF) [35].

To construct an easy-to-prepare and universal ^{10}B delivery system for BNCT, BSH-encapsulated liposomes were prepared with nickel lipid, and EGFR antibodies were conjugated to the liposomes using the antibody affinity motif of protein A (ZZ) as an adaptor (Fig. **1A**). The His-tag at the C-terminus of the recombinant ZZ was used not only for purification, but also for interaction with Ni-NTA (Nickel-[N-(5-amino-1-carboxypentyl)-iminodiacetic acid]) lipids [47]. In animals bearing U87ΔEGFR glioma cells, a high ^{10}B level was obtained in the tumor after the intravenous administration of the BSH-encapsulated nickel-immunoliposomes compared to

liposomes (Fig.**2A**). Immunohistochemical (IHC) analysis using an anti-BSH monoclonal antibody also revealed that BSH was delivered effectively into the cancerous part of the brain (Fig.**2B**). To extend the function of immunoliposomes in boron delivery systems, a fusion protein composed of ZZ and *Gaussia princeps* luciferase (GLase) for antibody binding and imaging, was expressed. Immunoliposomes were constructed with DSPE-PEG-MAL (N-[(3-maleimide-1-oxopropyl)aminopropyl polyethyleneglycol-carbamyl] distearoylphosphatidyl-ethanolamine) for covalent GLase-ZZ conjugation (Fig. **1B**). Fluorescence dye (8-Hydroxypyrene-1,3,6-trisulfonic acid trisodium salt, HPTS)-encapsulated immunoliposomes conjugated with ZZ-GLase showed more fluorescence in U87 ΔEGFR cells. *In vivo*, HPTS fluorescence and strong bioluminescence could be detected at the tumor site, suggesting that the new biofunctional immunoliposome system provides the potential for drug delivery and imaging *in vivo* [48].

2.3. Liposomes in Gene Therapy

Cationic liposomes have the potential to effectively deliver DNA or RNA and are one of the most promising vectors for human gene therapy. Cationic liposomes are usually formed with positively charged lipids in combination with a neutral helper lipid such as DOPE or cholesterol [49,50].

As nonviral vectors, liposome-based gene delivery systems combine the advantages of safety and the potential for tissue-selective drug targeting. Numerous cationic liposomes have been developed for gene transfection, and some have been used in gene therapy in preclinical and clinical trials [51]. For the application of cationic liposome-mediated gene delivery, it is necessary to identify more potent liposomal formulations, because assays *in vitro* are not always predictive, and the relative efficacy of different formulations depends on the site at which the formulation is administered. Nu-

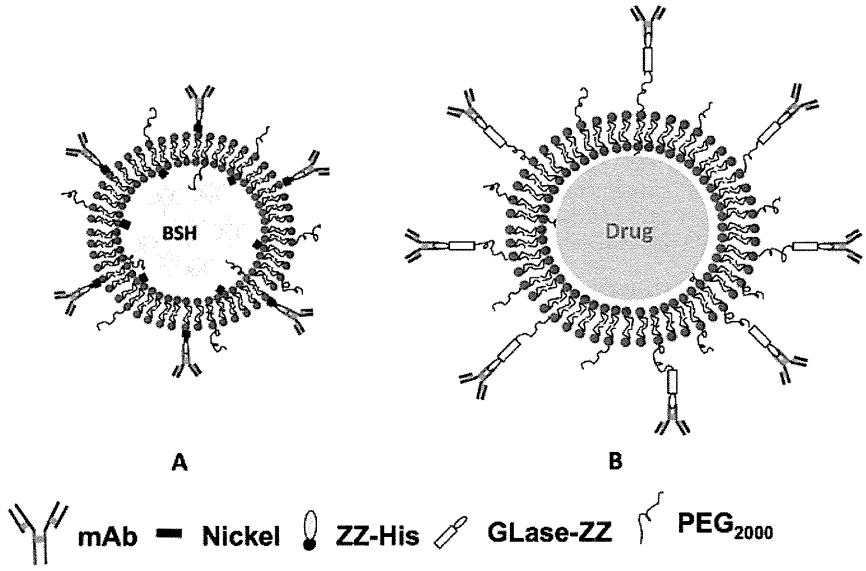

Fig. (1). Scheme of the immunoliposomes. (**A**) Nickel-immunoliposome (**B**) Bifunctional immunoliposome.

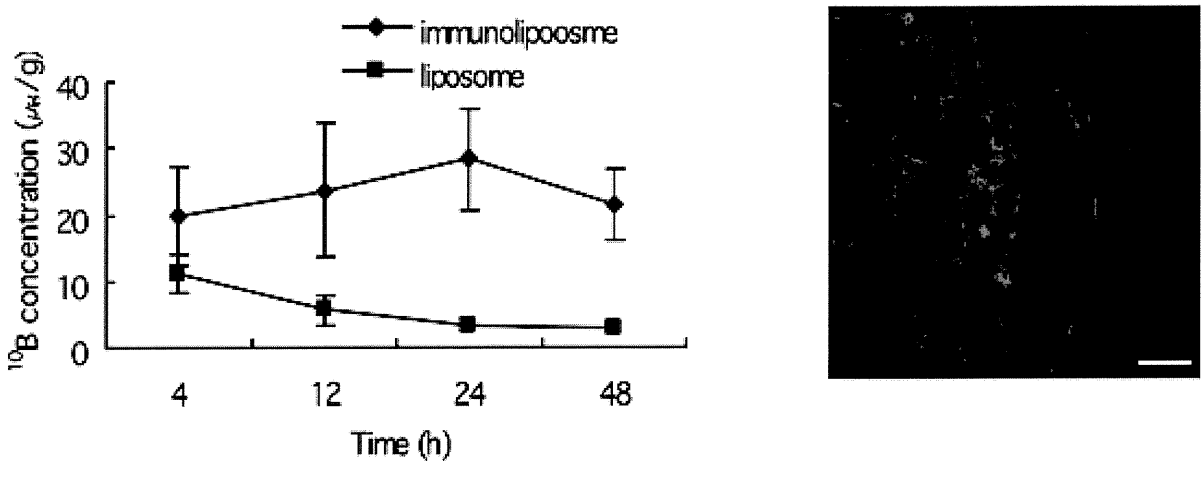

Fig. (2). Targeted boron delivery using nickel-immunoliposomes (**A**) Time course of ^{10}B's distribution in tumors. ^{10}B concentrations were measured after 400 μL of immunoliposome or liposome was injected into tumor-bearing mice *via* a tail vein at a dose of 35 mg ^{10}B/kg. (**B**) IHC analysis of BSH's distribution in tumors. The slice was prepared 4 h post immunoliposome injection. Anti-BSH mouse mAb and Cy3-conjugated mouse IgG were used as the primary and secondary antibody. Bar = 200 μm.

merous reports have described cancer gene therapy by direct intratumoral injection using DNA-cationic liposome complexes, and formulations that are active in one tissue may not be optimally active by a different route of administration [52].

Studies on clinical gene therapies for malignant gliomas using liposomal delivery systems are very few. Suicide gene (the herpes simplex virus thymidine kinase, HSV-tk) and cytokine gene therapies are performed for malignant gliomas [53,54]. Cationic liposome-mediated interferon-beta (*IFN-β*) gene transfer has been found to induce regression of experimental glioma. Wakabayashi T *et al.* performed a pilot clinical trial to evaluate the safety and effectiveness of IFN-β gene therapy in five patients with high-grade glioma. The surgical margin of the resection cavity was infiltrated with 1 ml of liposomes containing the human IFN-β gene. Two patients showed more than a 50% reduction while others had stable disease 10 weeks after treatment initiation [55].

Zhang *et al.* [56] encapsulated anti-luciferase shRNA expression plasmids inside PEGylated immunoliposomes (PILs). The PILs are delivered across the blood-brain barrier and across the tumor cell membrane *in vivo* by a mAb to the rat transferrin receptor (TfR). The TfR mAb-targeting PILs inhibited luciferase gene expression in brain cancer cells by 90%.

3. OTHER NANOPARTICLES

3.1. Polymeric Nanoparticles

From "Starburst" dendrimeric polymers to self-assembled polymeric micelles, polymeric nanoparticles have been developed to encapsulate drug molecules for DDS for many decades [57]. Typical biodegradable nano-DDS consist of colloidal polymeric nanoparticles with drug molecules that are encapsulated, mixed, absorbed, or attached onto the polymer matrix [58]. Poly (D,L - lactide-co-glycolide) (PLGA) carrier nanoparticles have been shown to intracellularly deliver therapeutic molecules for sustained drug release. Paclitaxel-loaded biodegradable PLGA foams with a microporous matrix were fabricated by a pressure quenching approach to provide a sustained drug release. These foams could be employed as potential implants for post-surgical chemotherapy against malignant glioma [59]. The encapsulation efficiency for paclitaxel-loaded PLGA nanofibers is more than 90% and *in vitro* efficacy tests against C6 glioma cells indicate that they may be promising drug delivery devices for the treatment of GBM [60].

Block-copolymer micelles composed of PEG–poly(α,β-aspartic acid) and PEG–poly(β-benzyl-L-aspartate) are additional classes of polymeric nanoparticles. They are formed spontaneously in aqueous solutions through the process of self-assembly when the polymer concentration is above the critical micellar concentration [61]. These molecular self-assembled polymeric micelles have exhibited high aqueous solubility and stability [10]. Drug molecules are loaded within the micellar core either through the physical encapsulation process or by direct conjugation. Passive nano-DDS delivery to diseased sites was achieved due to enhanced permeation and retention effects. Biomolecules such as peptides, oligonucleotides, oligosaccharides, and antibodies are all potential candidates for active targeting. Lf (lactoferrin) receptor (LfR) has been demonstrated on the BBB in different species and involved in the transport of Lf across the BBB *in vitro* and *in vivo* [62]. PEG–poly (lactide) (PEG–PLA) nanoparticles were constructed to conjugate with Lf and a lipophilic fluorescent dye, coumarin-6, was incorporated. Uptake by a mouse brain endothelial cell line (bEnd.3 cell line) *in vitro* and localization in brain tissue sections were visualized by fluorescence microscopy *in vivo* compared with pegylated nanoparticles [63].

The RGD (Arg-Gly-Asp) sequence has been identified as an essential binding motif to facilitate interaction between drug delivery systems including micelles and some integrins which connect cells to proteins of the extracellular matrix [64]. Among these integrins, αv integrin receptors, which are found to be highly expressed on activated endothelial cells and tumor cells (such as U87MG glioblastoma cells) but not in resting endothelial cells and most normal organ systems, constitute a potential target for tumor imaging and therapy. Zhan *et al.* [65] synthesized c(RGDyK)-modified PEG-PLA micelles to encapsulate paclitaxel. c(RGDyK)-PEG-PLA micelles accumulated in the subcutaneous tumor tissue, and when loaded with paclitaxel (c(RGDyK)-PEG-PLA-paclitaxel), exhibited the strongest tumor growth inhibition, suggesting c(RGDyK)-PEG-PLA micelles to be a potential drug delivery system in the treatment of integrin αvβ3 over-expressing glioblastomas.

Intravenously injected doxorubicin-loaded poly(n-butyl cyanoacrylate) nanoparticles coated with polysorbate 80 (Tween®) have been shown to prolong survival in rats with intracranially transplanted glioblastomas from the cell line 101/8 [17]. In addition, polybutyl cyanoacrylate nanoparticles coated with poloxamer 188 (Pluronic®) considerably enhanced the anticancer effect of doxorubicin against intracranial glioblastomas in rats [66].

3.2. Metallic Nanoparticles for Imaging and Treatment of Brain Tumors

Metallic nanoparticles have been used as contrast probes for imaging, diagnostics, and therapeutic platforms in brain tumors. Due to the relatively high resolution and good contrast between healthy and diseased tissues, nanoparticle-based MRI is currently used in both basic research and clinical settings. Superparamagnetic particle conjugates have been used to locate brain tumors earlier and to target the tumors more accurately [67]. Iron oxide nanoparticle-based MRI contrast agents show excellent potential for imaging in the CNS. Depending on the size of the nanoparticles, the iron oxide contrast agents are termed superparamagnetic iron oxides (SPIO) or ultra-small superparamagnetic iron oxides (USPIO). SPIO have proved to be an important tool for enhancing magnetic resonance contrast, allowing researchers to monitor not only anatomical changes, but physiological and molecular changes as well. Dextran-coated USPIO have also been delivered to human brain tumors with Sinerem® (a contrast agent for MRI) and showed gradual signal enhancement [68,69].

Magnetic nanoparticles can be used as a homing device to deliver drugs and contrast agents to a site by controlling the external magnetic field [70]. Magnetic nanoparticles have also been used for the transfection of DNA sequences [71], a process termed magnetofection. Themotherapy of GBM using magnetic nanoparticles is a recognized procedure and is often combined with chemotherapy. Selected heating of the brain tumor can be achieved by magnetic nanoparticles localized to the tumor and thermoablation is based on magnetic field-induced excitation of biocompatible superparamagnetic nanoparticles. In a rat tumor model with RG-2-cells implanted into the brain, thermotherapy was performed by exposing them to an alternating magnetic field following injection of aminosilane-coated iron oxide nanoparticles. Thermotherapy with aminosilane-coated nanoparticles led to up to 4.5-fold prolongation of survival [72]. Thermotherapy using magnetic nanoparticles was tolerated well by patients with minor or no side effects. A median maximum intratumoral temperature of 44.6°C was recorded with regression of tumor growth, indicating that this therapy can be used safely and effectively in human GBM [73].

3.3. Bionanocapsules

Bio-nanocapsules (BNCs) are virus-like empty nanoparticles made of phospholipids and envelope proteins derived from the hepatitis B virus (HBV). BNCs are recombinant yeast-derived hepatitis B virus surface antigen particles, which have been used as a recombinant hepatitis B vaccine for the last 20 years throughout the world, suggesting that BNCs are safe DDS.

If BNCs can be specifically delivered to brain tumors, they might be promising carriers of anti-tumor drugs to brain tumors and be effective for the treatment of brain tumors. The major component of BNC is the longest form of the envelope protein (L protein) and contains the preS1 region [74]. This region is the determinant of specific infectivity in human hepatocytes for BNC as well as HBV. Since it does not contain a viral genome, BNC is nontoxic to cells *in vitro* and safe *in vivo* especially to humans when used as vaccines. BNC is now being developed as a novel drug delivery vector capable of the specific delivery of genes, proteins and pharmaceutical drugs to human hepatocytes with high efficacy. When the pre-S1 region is replaced with other targeting moieties or biorecognition molecules, such as antibodies, receptors, and ligands, the specificity of BNC can be altered and may be applicable for the retargeting of BNCs to specific cells or tissues other than liver tissue [75].

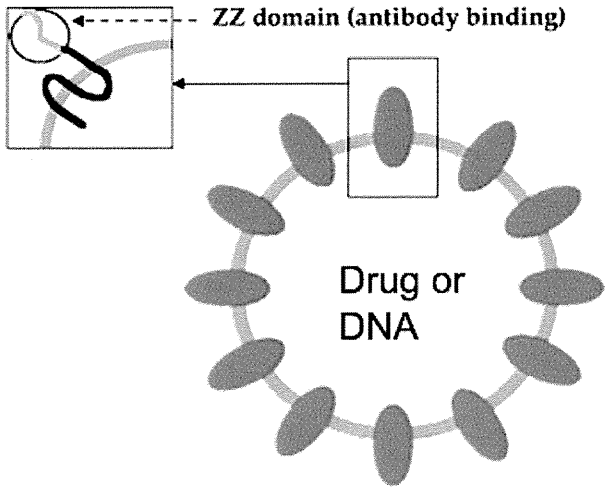

Fig. (3). Illustration of Bionanocapsules (ZZ-BNC).

To extend the targeting range of BNCs, the pre-S1 peptide on the surface of BNCs was replaced with the antibody affinity motif of protein A (ZZ), resulting in ZZ-BNC (Fig. **3**). ZZ-BNC bound with anti-human EGFR antibody was specifically delivered to cultured glioblastoma Gli36 cells overexpressing EGFR but not normal glial cells. The targeting of glioma was also confirmed in a mouse brain tumor model [76]. The fluospheres could be specifically delivered to Gli36 cells by the active targeting of zz-BNCs with anti-EGFR antibodies.

3.4. Multifunctional Nanoparticles

Multi-functionality provides advantages to nanoparticle-based DDS for the cancer-specific delivery of therapeutic or imaging agents. A universal nanoparticle-based platform can simultaneously detect, image, and deliver therapeutic compounds to tumor cells.

Tumor-specific accumulation of nanoparticles provides not only the means for drug delivery to the tumor, but also an opportunity to further conjugate a metallic core or shell for optical imaging or MRI in tumor diagnostics, guided hyperthermia therapy, and guided radiation therapy [77]. The use of targeted multifunctional nanoparticles can combine diagnosis with the treatment of brain tumors, such as the encapsulation of photodynamic therapy (PDT) agents (Photofrin®) with imaging agents (iron oxide) in polymeric nanoparticles. PDT involves the delivery of photosensitizers such as Photofrin® to tumors, combined with local excitation by the appropriate wavelength of light, resulting in the production of singlet oxygen and other reactive oxygen species. These initiate apoptosis and cytotoxicity in many types of tumors, with minimal systemic toxicity. PDT is more selective and less toxic than chemotherapy because the drug is not activated until the light is delivered. Reddy *et al.* linked a vascular-targeting peptide on the surface of nanoparticles encapsulated with photosensitizers and iron oxide. Significant MRI contrast enhancement was observed in glioma-bearing rats following intravenous administration. The survival rate in PDT-treated mice was also improved compared with controls [78].

For *in vitro* and *in vivo* optical imaging, semiconductor quantum dots (QDs) have recently emerged as a promising alternative to fluorescent markers; their superior brightness and photostability make them excellent candidates in the development of trackable multifunctional agents. Peptides (RGD) and antibodies have been conjugated to QDs for targeting in living subjects. Weng *et al.* constructed QD-conjugated immunoliposome-based nanoparticles (QD-ILs) with anti-HER2 scFv. Localization of QD-ILs at tumor sites was visualized by *in vivo* fluorescence imaging in nude mice bearing MCF-7/HER2 xenografts. Doxorubicin-loaded QD-ILs also showed efficient anticancer activity [79].

Mulder *et al.* used QDs conjugated to paramagnetic and pegylated lipids for combined fluorescence and MRI [80]. The specificity and sensitivity of the bimodal nanoparticles covalently linking RGD peptides were assessed and confirmed in cultured endothelial cells. Potentially, such nano-DDS could be used for the diagnosis of brain tumors with enhanced MRI imaging, and fluorescence emission from QDs could help physicians perform real-time tumor resection using optical guidance with encapsulated drug molecules providing post-surgical adjuvant therapy. Thus, drug molecules conjugated to these heterogeneous nanoparticles can provide additional functionalities. However, a disadvantage of QDs and metallic nanoparticles is known to be less biocompatible. For example, breakdown of semiconductor QDs composed of heavy metal ions could result in release of potent heavy metal ions such as cadmium ions and cause significant hepatotoxic effect in liver cells [81]. Compared with liposomes and polymers, there are many years away for QDs from reaching clinical trials.

The complexity of brain tumors also provides a challenge to constructing more effective multifunctional nanoparticles. Targeting brain tumors more accurately is the most important step. Till now, tumor surface markers used for targeted delivery include: EGFR; transferrin receptor; folate receptor; integrin $\alpha v\beta 3$; extracellular matrix (ECM) glycoproteins [82]. The targeting molecules for the corresponding markers are EGF or anti-EGFR antibody, transferrin; floate; RGD, and sulfatide, separately. Recently, brain tumor stem cells (BTSCs) were found to have extraordinary potential to initiate and maintain brain tumors, [83,84]. BTSCs are the driving force of tumor growth, making tumors resistant to radiotherapy and chemotherapy. Therefore, it is important to eliminate BTSCs for the treatment of brain tumors [85]. Identification of the markers of BTSCs will provide a good target to kill tumor cells in the early stage, providing a better therapeutic effect. CD133 is one widely accepted molecular marker expressed in BTSCs but not in bulk tumor cells [83] and can be manipulated as a therapeutic target for nanoparticles to eliminate BTSCs.

4. CONCLUSIONS

Due to non-toxicity and convenient modification, the utilization of nanoparticles as potential targeted vectors for delivering contrast or therapeutic agents to brain tumors has the following advantages [4]: 1. Nanoparticles modified with targeting molecules can pass through the BBB and achieve the delivery of large amounts of therapeutic or imaging agents to tumor cells, although the selective delivery of nanoparticles to tumor is sometimes achieved due to the leaky tumor vasculature, which is known as the EPR effect [86]. 2. A hydrophilic coating and the nanoparticle matrix provide reduced uptake by the RES and provide protection of active agents from environmental degradation, resulting in increased delivery of the nanoparticles to tumor sites and reduced toxicity. 3. The nanoparti-

cles can alleviate the problems posed by the multi-drug resistance (MDR) of cancer cells against many drugs and reduce immunogenicity and side effects.

The future of nanoparticles lies in multifunctional nanoplatforms, which combine both therapeutic components and multimodality imaging. The development of nanoparticle-based DDS could provide efficient, specific *in vivo* drug delivery without systemic toxicity, and the dose delivered as well as the therapeutic efficacy can be accurately measured noninvasively over time. Although conventional nanoparticles such as liposomes and polymers have been approved for clinical use, there is still a long way to go before newer classes of nanoparticles composed of QDs or metallic particles become a clinical reality. Much remains to be done and many factors need to be optimized, among which are biocompatibility, *in vivo* targeting efficacy, pharmacokinetics, and acute/chronic toxicity.

There are also some concerns about the biosafety and possible side effects of using nanopaticles. Nanotoxicology has emerged as a new area for studying the undesirable effects of nanoparticles [87]. First, the toxicity may come from the material itself, such as CdSe/CdTe in QDs. The modification of QDs renders them more biologically inert for future clinical application. Nanoparticle-based drug delivery for solid brain tumors still has a long way to go, but the strong need for more effective chemotherapeutics will continue to motivate studies on nanoparticles. With the capacity to provide effective targeting, high sensitivity, less toxicity and flexibility, nanoparticle-based drug delivery systems will eventually be able to impact disease diagnosis and patient therapy.

ACKNOWLEDGEMENTS

This work was supported by a Grant-in-aid for Scientific Research from the Ministry of Education, Science, Sports and Culture of Japan and by National Natural Science Foundation of China (No. 81071248).

REFERENCES

[1] DeAngelis, L.M. Brain tumors. *N. Engl. J. Med.,* **2001**, *344*, 114-123.

[2] van Rij, C.M.; Wilhelm, A.J.; Sauerwein, W.A.; van Loenen, A.C. Boron neutron capture therapy for glioblastoma multiforme. *Pharm. World Sci.,* **2005**, *27*, 92-95.

[3] Bao, S.; Wu, Q.; McLendon, R.E.; Hao, Y.; Shi, Q.; Hjelmeland, A.B.; Dewhirst, M.W.; Bigner, D.D.; Rich, J.N. Glioma stem cells promote radioresistance by preferential activation of the DNA damage response. *Nature*, **2006**, *444*, 756-760.

[4] Koo, Y.E.; Reddy, G.R.; Bhojani, M.; Schneider, R.; Philbert, M.A.; Rehemtulla, A.; Ross, B.D.; Kopelman, R. Brain cancer diagnosis and therapy with nanoplatforms. *Adv. Drug Deliv. Rev.,* **2006**, *58*, 1556-1577.

[5] Allen, T.M.; Cullis, P.R. Drug delivery systems: entering the mainstream. *Science*, **2004**, *303*, 1818-1822.

[6] Couvreur, P.; Kante, B.; Crislain, L.; Roland, M.; Speiser, P. Toxicity of polyalkylcyanoacrylate nanoparticles II: doxorubicin-loaded nanoparticles. *J. Pharm. Sci.*, **1982**, *71*, 790-792.

[7] Beck, P.; Kreuter, J.; Reszka, R.; Fichtner, I. Influence of polybutylcyanoacrylate nanoparticles and liposomes on the efficacy and toxicity of anticancer drug mitoxantrone in murine tumour models. *J. Microencapsul.*, **1993**, *10*, 101-114.

[8] Lockman, P.R.; Mumper, R.J.; Khan, M.A.; Allen, D.D. Nanoparticle technology for drug delivery across the blood-brain barrier. *Drug Dev. Ind. Pharm.*, **2002**, *28*, 1-13.

[9] Yoon, T.J.; Kim, J.S.; Kim, B.G.; Yu, K.N.; Cho, M.H.; Lee, J.K. Multifunctional nanoparticles possessing a "magnetic motor effect" for drug or gene delivery. *Angew. Chem. Int. Ed. Engl.*, **2005**, *44*, 1068-1071.

[10] Kataoka, K.; Harada, A.; Nagasaki, Y. Block copolymer micelles for drug delivery: design, characterization and biological significance. *Adv. Drug Deliv. Rev.*, **2001**, *47*, 113-131.

[11] Panyam, J.; Labhasetwar, V. Biodegradable nanoparticles for drug and gene delivery to cells and tissue. *Adv. Drug Deliv. Rev.*, **2003**, *55*, 329-347.

[12] Batist, G.; Ramakrishnan, G.; Rao, C.S.; Chandrasekharan, A.; Gutheil, J.; Guthrie, T.; Shah, P.; Khojasteh, A.; Nair, M.K.; Hoelzer, K.; Tkaczuk, K.; Park, Y.C.; Lee, L.W. Reduced cardiotoxicity and preserved antitumor efficacy of liposome-encapsulated doxorubicin and cyclophosphamide compared with conventional doxorubicin and cyclophosphamide in a randomized, multicenter trial of metastatic breast cancer. *J. Clin. Oncol.*, **2001**, *19*, 3439-3441.

[13] Shenoy, D.; Little, S.; Langer, R.; Amiji, M. Poly(ethylene oxide)- modified poly(β-amino ester) nanoparticles as a pH-sensitive system for tumor-targeted delivery of hydrophobic drugs: Part 2. *In vivo* distribution and tumor localization studies. *Pharm. Res.*, **2005**, *22*, 2107-2114.

[14] Maeda, H.; Wu, J.; Sawa, T.; Matsumura, Y.; Hori, K. Tumor vascular permeability and the EPR effect in macromolecular therapeutics: a review. *J. Control Release*, **2000**, *65*, 271-284.

[15] Sengupta, S.; Eavarone, D.; Capila, I.; Zhao, G.; Watson, N.; Kiziltepe, T.; Sasisekharan, R. Temporal targeting of tumour cells and neovasculature with a nanoscale delivery system. *Nature*, **2005**, *436*, 568-572.

[16] Kingsley, J.D.; Dou, H.; Morehead, J.; Rabinow, B.; Gendelman, H.E.; Destache, C.J. Nanotechnology: a focus on nanoparticles as a drug delivery system. *J. Neuroimmune Pharmacol.*, **2006**, *1*, 340-350.

[17] Kreuter, J. Nanoparticulate systems for brain delivery of drugs. *Adv. Drug Deliv. Rev.*, **2001**, *47*, 65-81.

[18] Chen, Y.; Dalwadi, G.; Benson, H.A. Drug delivery across the blood-brain barrier. *Curr. Drug Deliv.*, **2004**, *1*, 361-376.

[19] Schlageter, K.E.; Molnar, P.; Lapin, G.D.; Groothuis, D.R. Microvessel organization and structure in experimental brain tumors: Microvessel populations with distinctive structural and functional properties. *Microvasc. Res.*, **1999**, *58*, 312-328.

[20] Vajkoczy, P.; Menger, M.D. Vascular microenvironment in gliomas. *Cancer Treat. Res.*, **2004**, *117*, 249-262.

[21] Reddy, J.A.; Allagadda, V.M.; Leamon, C.P. Targeting therapeutic and imaging agents to folate receptor positive tumors. *Curr. Pharm. Biotechnol.*, **2005**, *6*, 131-150.

[22] Cascante, M.; Centelles, J.J.; Veech, R.L.; Lee, W.N.; Boros, L.G. Role of thiamin (vitamin B-1) and transketolase in tumor cell proliferation. *Nutr. Cancer*, **2000**, *36*, 150-154.

[23] Park, J.W.; Benz, C.C.; Martin, F.J. Future directions of liposome- and immunoliposome-based cancer therapeutics. *Semin. Oncol.*, **2004**, *31*, 196-205.

[24] Maurer, N.; Fenske, D.B.; Cullis, P.R. Developments in liposomal drug delivery systems. *Expert Opin. Biol. Ther.*, **2001**, *1*, 923-947.

[25] Jiang, W.; Kim, B.Y.; Rutka, J.T.; Chan, W.C. Advances and challenges of nanotechnology-based drug delivery systems. *Expert Opin. Drug Deliv.*, **2007**, *4*, 621-633.

[26] Carlsson, J.; Kullberg, E.B.; Capala, J.; Sjöberg, S.; Edwards, K.; Gedda, L. Ligand liposomes and boron neutron capture therapy. *J. Neurooncol.*, **2003**, *62*, 47-59.

[27] Sofou, S.; Sgouros, G. Antibody-targeted liposomes in cancer therapy and imaging. *Expert Opin. Drug Deliv.*, **2008**, *5*, 189-204.

[28] Maruyama, K. PEG-immunoliposome. *Biosci. Rep.*, **2002**, *22*, 251-266.

[29] Hansen, C.B.; Kao, G.Y.; Moase, E.H.; Zalipsky, S.; Allen, T.M. Attachment of antibodies to sterically stabilized liposomes-evaluation, comparison and optimization of coupling procedures. *Biochim. Biophys. Acta*, **1995**, *1239*, 133-144.

[30] Allen, T.M.; Brandeis, E.; Hansen, C.B.; Kao, G.Y.; Zalipsky, S. A new strategy for attachment of antibodies to sterically stabilized liposomes resulting in efficient targeting to cancer-cells. *Biochim. Biophys. Acta*, **1995**, *1237*, 99-108.

[31] Sapra, P.; Tyagi, P.; Allen, T.M. Ligand-targeted liposomes for cancer treatment. *Curr. Drug Deliv.*, **2005**, *2*, 369-381.

[32] Park, J.W.; Hong, K.; Kirpotin, D.B.; Colbern, G.; Shalaby, R.; Baselga, J.; Shao, Y.; Nielsen, U.B.; Marks, J.D.; Moore, D.; Papahadjopoulos, D.; Benz, C.C. Anti-HER2 immunoliposomes: enhanced efficacy attributable to targeted delivery. *Clin. Cancer Res.*, **2002**, *8*, 1172-1181.

[33] Gabizon, A.; Papahadjopoulos, D. The role of surface charge and hydrophilic groups on liposome clearance *in vivo*. *Biochim. Biophys. Acta,* **1992**, *1103*, 94-100.

[34] Unezaki, S.; Maruyama, K.; Takahashi, N.; Koyama, M.; Yuda, T.; Suginaka, A.; Iwatsuru, M. Enhanced delivery and antitumor activity of doxorubicin using long-circulating thermosensitive liposomes containing amphipathic polyethylene glycol in combination with local hyperthermia. *Pharm. Res.*, **1994**, *11*, 1180-1185.

[35] Friedman, H.S.; Bigner, D.D. Glioblastoma multiforme and the epidermal growth factor receptor. *N. Engl. J. Med.*, **2005**, *353*, 1997-1999.

[36] Schwechheimer, K.; Huang, S.; Cavenee, W.K. EGFR gene amplification-rearrangement in human glioblastomas. *Int. J. Cancer*, **1995**, *62*, 145-148.

[37] Sauter, G.; Maeda, T.; Waldman, F.M.; Davis, R.L.; Feuerstein, B.G. Patterns of epidermal growth factor receptor amplification in malignant gliomas. *Am. J. Pathol.*, **1996**, *148*, 1047-1053.

[38] Ishida, T.; Iden, D.L.; Allen, T.M. A combinatorial approach to producing sterically stabilized (Stealth) immunoliposomal drugs. *FEBS Lett.*, **1999**, *460*, 129-133.

[39] Iden, D.L.; Allen, T.M. *In vitro* and *in vivo* comparison of immunoliposomes made by conventional coupling techniques with those made by a new post-insertion approach. *Biochim. Biophys. Acta*, **2001**, *1513*, 207-216.

[40] Caruso, G.; Raudino, G.; Caffo, M.; Alafaci, C.; Granata, F.; Lucerna, S.; Salpietro, F.M.; Tomasello, F. Nanotechnology Platforms in Diagnosis and Treatment of Primary Brain Tumors. *Recent. Pat. Nanotechnol.*, **2010**, *4*, 119-124.

[41] Hofheinz, R.D.; Gnad-Vogt, S.U.; Beyer, U.; Hochhaus, A. Liposomal encapsulated anti-cancer drugs. *Anticancer Drugs*, **2005**, *16*, 691-707.

[42] Orringer, D.A.; Koo, Y.E.; Chen, T.; Kopelman, R.; Sagher, O.; Philbert, M.A. Small solutions for big problems: the application of nanoparticles to brain tumor diagnosis and therapy. *Clin. Pharmacol. Ther.*, **2009**, *85*, 531-534.

[43] Barth, R.F.; Coderre, J.A.; Vicente, M.G.; Blue, T.E. Boron neutron capture therapy of cancer: current status and future prospects. *Clin. Cancer Res.*, **2005**, *11*, 3987-4002.

[44] Yanagië, H.; Ogata, A.; Sugiyama, H.; Eriguchi, M.; Takamoto, S.; Takahashi, H. Application of drug delivery system to boron neutron capture therapy for cancer. *Expert Opin. Drug Deliv.*, **2008**, *5*, 427-443.

[45] Pan, X.Q.; Wang, H.; Lee, R.J. Boron delivery to a murine lung carcinoma using folate receptor-targeted liposomes. *Anticancer Res.*, **2002**, *22*, 1629-1633.

[46] Doi, A.; Kawabata, S.; Iida, K.; Yokoyama, K.; Kajimoto, Y.; Kuroiwa, T.; Shirakawa, T.; Kirihata, M.; Kasaoka, S.; Maruyama, K.; Kumada, H.; Sakurai, Y.; Masunaga, S.; Ono, K.; Miyatake, S. Tumor specific targeting of sodium borocaptate (BSH) to malignant glioma by transferrin-PEG liposomes: a modality for boron neutron capture therapy. *J. Neurooncol.*, **2008**, *87*, 287-294.

[47] Feng, B.; Tomizawa, K.; Michiue, H.; Miyatake, S.; Han, X.J.; Fujimura, A.; Seno, M.; Kirihata, M.; Matsui, H. Delivery of sodium borocaptate to glioma cells using immunoliposome conjugated with anti-EGFR antibodies by ZZ-His. *Biomaterials*, **2009**, *30*, 1746-1755.

[48] Feng, B.; Tomizawa, K.; Michiue, H.; Han, X.J.; Miyatake, S.; Matsui, H. Development of a bifunctional immunoliposome system for combined drug delivery and imaging *in vivo*. *Biomaterials*, **2010**, *31*, 4139-4145.

[49] Martin, B.; Sainlos, M.; Aissaoui, A.; Oudrhiri, N.; Hauchecorne, M.; Vigneron, J.P.; Lehn, J.M.; Lehn, P. The design of cationic lipids for gene delivery. *Curr. Pharm. Des.*, **2005**, *11*, 375-394.

[50] Wasungu, L.; Hoekstra, D. Cationic lipids, lipoplexes and intracellular delivery of genes. J. Control Release, **2006**,116, 255-264.

[51] Gao, X.; Huang, L. Cationic liposome-mediated gene transfer. *Gene Ther.*, **1995**, *2*, 710-722.

[52] Felgner, P.L. Improvements in cationic liposomes for *in vivo* gene transfer. *Hum. Gene Ther.*, **1996**, *7*, 1791-1793.

[53] Voges, J.; Weber, F.; Reszka, R.; Sturm, V.; Jacobs, A.; Heiss, W.D.; Wiestler, O.; Kapp, J.F. Clinical protocol. Liposomal gene therapy with the herpes simplex thymidine kinase gene/ganciclovir system for the treatment of glioblastoma multiforme. *Hum. Gene Ther.*, **2002**, *13*, 675-685.

[54] Yoshida, J.; Mizuno, M.; Clinical gene therapy for brain tumors. Liposomal delivery of anticancer molecule to glioma. *J. Neurooncol.*, **2003**, *65*, 261-267.

[55] Yoshida, J.; Mizuno, M.; Fujii, M.; Kajita, Y.; Nakahara, N.; Hatano, M.; Saito, R.; Nobayashi, M.; Wakabayashi, T. Human gene therapy for malignant gliomas (glioblastoma multiforme and anaplastic astrocytoma) by *in vivo* transduction with human interferon beta gene using cationic liposomes. *Hum. Gene Ther.*, **2004**, *15*, 77-86.

[56] Zhang, Y.; Boado, R..J.; Pardridge, W.M. *In vivo* knockdown of gene expression in brain cancer with intravenous RNAi in adult rats. *J. Gene Med.*, **2003**, *5*, 1039-1045.

[57] Lavasanifar, A.; Samuel, J.; Kwon, G.S. Poly(ethylene oxide)- block -poly(L -amino acid) micelles for drug delivery. *Adv. Drug Deliv. Rev.*, **2002**, *54*, 169-190.

[58] Sahoo, S.K.; Labhasetwar, V. Nanotech approaches to drug delivery and imaging. *Drug Discov. Today*, **2003**, *8*, 1112-1120.

[59] Ong, B.Y.; Ranganath, S.H.; Lee, L.Y.; Lu, F.; Lee, H.S.; Sahinidis, N.V.; Wang, C.H. Paclitaxel delivery from PLGA foams for controlled release in post-surgical chemotherapy against glioblastoma multiforme. *Biomaterials*, **2009**, *30*, 3189-3196.

[60] Xie, J.; Wang, C.H. Electrospun micro- and nanofibers for sustained delivery of paclitaxel to treat C6 glioma *in vitro*. *Pharm. Res.*, **2006**, *23*, 1817-1826.

[61] Haag, R. Supramolecular drug-delivery systems based on polymeric core-shell architectures. *Angew. Chem. Int. Ed. Engl.*, **2004**, *43*, 278-282.

[62] Huang, R.Q.; Ke, W.L.; Qu, Y.H.; Zhu, J.H.; Pei, Y.Y.; Jiang, C. Characterization of lactoferrin receptor in brain endothelial capillary cells and mouse brain. *J. Biomed. Sci.*, **2007**, *14*, 121-128.

[63] Hu, K.; Li, J.; Shen, Y.; Lu, W.; Gao, X.; Zhang, Q.; Jiang, X. Lactoferrin-conjugated PEG-PLA nanoparticles with improved brain delivery: *in vitro* and *in vivo* evaluations. *J. Control Release*, **2009**, *134*, 55-61.

[64] Schottelius, M.; Laufer, B.; Kessler, H.; Wester, H.J. Ligands for mapping alphavbeta3-integrin expression *in vivo*. *Acc. Chem. Res.*, **2009**, *42*, 969-980.

[65] Zhan, C.; Gu, B.; Xie, C.; Li, J.; Liu, Y.; Lu, W. Cyclic RGD conjugated poly(ethylene glycol)-co-poly(lactic acid) micelle enhances paclitaxel anti-glioblastoma effect. *J. Control Release*, **2010**,*143*, 136-142.

[66] Petri, B.; Bootz, A.; Khalansky, A.; Hekmatara, T.; Müller, R.; Uhl, R.; Kreuter, J.; Gelperina, S.; Chemotherapy of brain tumour using doxorubicin bound to surfactant-coated poly(butyl cyanoacrylate) nanoparticles: revisiting the role of surfactants. *J. Control Release*, **2007**, *117*, 51-58.

[67] Zhang, Y.; Sun, C.; Kohler, N.; Zhang, M. Self-assembled coatings on individual monodisperse magnetite nanoparticles for efficient intracellular uptake. *Biomed. Microdevices*, **2004**, *6*, 33-40.

[68] Neuwelt, E.A.; Várallyay, P.; Bagó, A.G.; Muldoon, L.L.; Nesbit, G.; Nixon, R. Imaging of iron oxide nanoparticles by MR and light microscopy in patients with malignant brain tumors, *Neuropathol. Appl. Neurobiol.*, **2004**, *30*, 456-471.

[69] Murillo, T.P.; Sandquist, C.; Jacobs, P.M.; Nesbit, G.; Manninger, S.; Neuwelt, E.A. Imaging brain tumors with ferumoxtran-10, a nanoparticle magnetic resonance contrast agent. *Therapy*, **2005**, *2*, 871-882.

[70] Xu, H.; Song, T.; Bao, X.; Hu, L. Site-directed research of magnetic nanoparticles in magnetic drug targeting. *J. Magn. Magn. Mater.*, **2005**, *293*, 514-519.

[71] Dobson, J. Gene therapy progress and prospects: magnetic nanoparticle-based gene delivery. *Gene Ther.*, **2006**, *13*, 283-287.

[72] Jordan, A.; Scholz, R.; Maier-Hauff, K.; van Landeghem, F.K.; Waldoefner, N.; Teichgraeber, U.; Pinkernelle, J.; Bruhn, H.; Neumann, F.; Thiesen, B.; von Deimling, A.; Felix, R. The effect of thermotherapy using magnetic nanoparticles on rat malignant glioma. *J. Neurooncol.*, **2006**, *78*, 7-14.

[73] Maier-Hauff, K.; Rothe, R.; Scholz, R.; Gneveckow, U.; Wust, P.; Thiesen, B.; Feussner, A.; von Deimling, A.; Waldoefner, N.; Felix, R.; Jordan, A. Intracranial thermotherapy using magnetic nanoparticles combined with external beam radiotherapy: results of a feasibility study on patients with glioblastoma multiforme. *J. Neurooncol.*, **2007**, *81*, 53-60.

[74] Yamada, T.; Iwasaki, Y.; Tada, H.; Iwabuki, H.; Chuah, M.K.; VandenDriessche, T.; Fukuda, H.; Kondo, A.; Ueda, M.; Seno, M.; Tanizawa, K.; Kuroda, S. Nanoparticles for the delivery of genes and drugs to human hepatocytes. *Nat. Biotechnol.*, **2003**, *21*, 885-890.

[75] Yu, D.; Fukuda, T.; Tuoya, Kuroda, S.; Tanizawa, K.; Kondo, A.; Ueda, M.; Yamada, T.; Tada, H.; Seno, M. Engineered bio-nanocapsules, the selective vector for drug delivery system. *IUBMB Life*, **2006**, *58*, 1-6.

[76] Tsutsui, Y.; Tomizawa, K.; Nagita, M.; Michiue, H.; Nishiki, T.; Ohmori, I.; Seno, M.; Matsui, H. Development of bionanocapsules targeting brain tumors. *J. Control Release*, **2007**, *122*, 159-164.

[77] van Vlerken, L.E.; Amiji, M.M. Multi-functional polymeric nanoparticles for tumour-targeted drug delivery. *Expert Opin. Drug Deliv.*, **2006**, *3*, 205-216.

[78] Reddy, G.R.; Bhojani, M.S.; McConville, P.; Moody, J.; Moffat, B.A.; Hall, D.E.; Kim, G.; Koo, Y.E.; Woolliscroft, M.J.; Sugai, J.V.; Johnson, T.D.; Philbert, M.A.; Kopelman, R.; Rehemtulla, A.; Ross, B.D. Vascular targeted nanoparticles for imaging and treatment of brain tumors. *Clin. Cancer Res.*, **2006**, *12*, 6677-6686.

[79] Weng, K.C.; Noble, C.O.; Papahadjopoulos-Sternberg, B.; Chen, F.F.; Drummond, D.C.; Kirpotin, D.B.; Wang, D.; Hom, Y.K.; Hann, B.; Park, J.W. Targeted tumor cell internalization and imaging of multifunctional quantum dot-conjugated immunoliposomes *in vitro* and *in vivo*. *Nano Lett.*, **2008**, *8*, 2851-2857.

[80] Mulder, W.J.; Koole, R.; Brandwijk, R.J.; Storm, G.; Chin, P.T.; Strijkers, G.J.; de Mello Donegá, C.; Nicolay, K.; Griffioen, A.W. Quantum dots with a paramagnetic coating as a bimodal molecular imaging probe. *Nano Lett.*, **2006**, *6*, 1-6.

[81] Derfus, A.M.; Chan, W.C.W.; Bhatia, S.N. Probing the cytotoxicity of semiconductor quantum dots. *Nano Lett.*, **2004**, *4*, 11-18.

[82] Shao, K.; Hou, Q.; Duan, W.; Go, M.L.; Wong, K.P.; Li, Q.T. Intracellular drug delivery by sulfatide-mediated liposomes to gliomas. *J. Control Release*, **2006**, *115*, 150-157.

[83] Singh, S.K.; Hawkins, C.; Clarke, I.D.; Squire, J.A.; Bayani, J.; Hide, T.; Henkelman, R.M.; Cusimano, M.D.; Dirks, P.B. Identification of human brain tumor initiating cells. *Nature*, **2004**, *432*, 396-401.

[84] Vescovi, A.L.; Galli, R.; Reynolds, B.A. Brain tumor stem cells. *Nat. Rev. Cancer*, **2006**, *6*, 425-436.

[85] Mao, X.G.; Zhang, X.; Zhen, H.N. Progress on potential strategies to target brain tumor stem cells. *Cell Mol. Neurobiol.*, **2009**, *29*, 141-155.

[86] Maeda, H. The enhanced permeability and retention (EPR) effect in tumor vasculature: the key role of tumor-selective macromolecular drug targeting, *Adv. Enzyme Regul.*, **2001**, *41*, 189-207.

[87] Kagan, V.E.; Bayir, H.; Shvedova, A.A. Nanomedicine and nanotoxicology: two sides of the same coin. *Nanomedicine*, **2005**, *1*, 313-316.

Received: ?????? 12, 2010 Revised: ?????? 25, 2010 Accepted: ????????? 14, 2010

Computed Tomography Imaging of Transferrin Targeting Liposomes Encapsulating Both Boron and Iodine Contrast Agents by Convection-Enhanced Delivery to F98 Rat Glioma for Boron Neutron Capture Therapy

Shiro Miyata, MD*
Shinji Kawabata, MD, PhD*
Ryo Hiramatsu, MD*
Atsushi Doi, MD, PhD*
Naokado Ikeda, MD, PhD*
Taro Yamashita, MD*
Toshihiko Kuroiwa, MD, PhD*
Satoshi Kasaoka, PhD‡
Kazuo Maruyama, PhD§
Shin-ichi Miyatake, MD, PhD*

*Department of Neurosurgery, Osaka Medical College, Osaka, Japan; ‡Faculty of Pharmaceutical Sciences, Hiroshima International University, Hiroshima, Japan; §Faculty of Pharmaceutical Sciences, Teikyo University, Tokyo, Japan.

Correspondence:
Shinji Kawabata, MD, PhD,
Department of Neurosurgery,
Osaka Medical College,
2-7 Daigaku-machi,
Takatsuki City,
Osaka 569-8686, Japan.
E-mail: neu046@poh.osaka-med.ac.jp.

Received, February 4, 2010.
Accepted, October 2, 2010.

WHAT IS THIS BOX?
A QR Code is a matrix barcode readable by QR scanners, mobile phones with cameras, and smartphones. **The QR Code above links to Supplemental Digital Content from this article.**

BACKGROUND: To achieve potent tumor-selective antitumor efficacy by boron neutron capture therapy (BNCT), it is important to have a significant differential uptake of 10B between tumor cells and normal cells. This should enable BNCT to reduce damage to normal tissues compared with other radiation therapies.

OBJECTIVE: To augment the therapeutic efficacy of BNCT, we used transferrin-conjugated polyethylene glycol (PEG) (TF-PEG) liposome encapsulating sodium borocaptate and lomeprol, an iodine contrast agent, with intratumoral convection-enhanced delivery (CED) in a rat glioma tumor model.

METHODS: The in vitro ^{10}B concentration of F98 rat glioma cells was determined by inductively coupled plasma atomic emission spectrometry after incubation with either TF-PEG or PEG liposomes. For in vivo biodistribution studies, ^{10}B concentrations within blood, normal brain tissue, and intracerebrally transplanted F98 cells were measured with inductively coupled plasma-atomic emission spectrometry after CED of the compounds, and computed tomography was performed at selected time intervals.

RESULTS: ^{10}B concentrations of F98 cultured glioma cells in vitro 6 hours after exposure to PEG and TF-PEG liposome were 16.1 and 51.9 ng^{10}B/10^6 cells, respectively. ^{10}B concentrations in F98 glioma tissue 24 hours after CED were 22.5 and 82.2 μg/g, by PEG and TF-PEG liposome, respectively, with lower ^{10}B concentrations in blood and normal brain. lomeprol provided vivid and stable enhanced computed tomography imaging of the transplanted tumor even 72 hours after CED by TF-PEG liposome. Conversely, tissue enhancement had already washed out at 24 hours after CED of the PEG liposomes.

CONCLUSION: The combination of TF-PEG liposome encapsulating sodium borocaptate and lomeprol and intratumoral CED enables not only a precise and potent targeting of boron delivery to the tumor tissue, but also the ability to follow the trace of boron delivery administered intratumorally by real-time computed tomography.

KEY WORDS: Boron neutron capture therapy, Computed tomography, Convection-enhanced delivery, Liposome, Transferrin

Neurosurgery 68:1380–1387, 2011 DOI: 10.1227/NEU.0b013e31820b52aa www.neurosurgery-online.com

ABBREVIATIONS: ^{10}B, boron-10; **BBB**, blood-brain barrier; **BDS**, boron delivery system; **BNCT**, boron neutron capture therapy; **BSH**, sodium borocaptate; **CED**, convection-enhanced delivery; **PEG**, polyethylene glycol; **TF-PEG**, transferrin-conjugated polyethylene glycol

Supplemental digital content is available for this article. Direct URL citations appear in the printed text and are provided in the HTML and PDF versions of this article on the journal's Web site (www.neurosurgery-online.com).

Therapeutic modalities such as stereotactic radiosurgery, intensity-modulated radiation therapy, particle radiation therapy, and novel therapeutic agents with molecular targeting have been developed to improve the prognosis of some types of brain tumors. However, over the past few decades, there has been little improvement in the prognosis of

patients with malignant gliomas because of the tumor's tendency to microscopically infiltrate the surrounding normal tissue. To overcome this infiltrative nature, it is necessary to selectively deliver a higher concentration of anticancer or radiation sensitizing agents into tumor tissue compared with the surrounding normal brain tissue. We are focusing on developing boron neutron capture therapy (BNCT) to achieve greater tumor-selective killing and therefore therapeutic efficacy.

At our institution, we have clinically applied BNCT since 2002 as an essential adjuvant therapy for patients with recurrent or newly diagnosed malignant gliomas[1-4] and have achieved superior outcomes compared with those by standard therapies using fractionated radiographic treatments.[5] BNCT is based on the nuclear capture and fission reactions that occur when boron-10 (^{10}B), a nonradioactive constituent of natural elemental boron, is irradiated with low-energy thermal neutrons to produce high-energy α particles and recoiling lithium-7 nuclei. These have high linear energy transfer and path lengths of approximately 9 and 5 μm, respectively, which theoretically allow them to discharge their energy within ^{10}B-containing cells.[6] Thus, to achieve potent tumor-selective antitumor efficacy, it is important to have a significant differential uptake of ^{10}B between tumor cells and normal cells. This should enable BNCT to reduce damage to normal tissues compared with other radiation therapies.

Today, clinically used sodium borocaptate (BSH) is transferred to brain tumors only through the disrupted blood-brain barrier (BBB), so it is difficult for BSH to reach regions that tumor cells invade microscopically where the BBB seems to be intact. On the other hand, boronophenylalanine, which transfers boron via L-type amino acid transporter, can deliver ^{10}B even in the infiltrating tumor cell population where the BBB is intact. However, some amounts of ^{10}B are inevitably taken into the normal cells by boronophenylalanine systemic administration. Moreover, the native heterogeneity of malignant gliomas interferes with the ability to accurately target the tumor. Recent reports have delineated boron delivery systems (BDSs) to improve molecular targeting of malignant gliomas.[7,8] Previously we reported on the effectiveness of transferrin-conjugated polyethylene glycol (PEG) (TF-PEG) liposome encapsulating BSH administered intravenously, with regard to its ability to target tumor cells and to increase the accumulation of ^{10}B in tumor tissue.[9]

To improve the efficacy of tumor targeting under systemic administration, the circulation time of a BDS in the blood needs to be lengthened. Unfortunately, systemic administration of a BDS increases the capture of ^{10}B-labeled molecules in the reticuloendothelial system of the liver and spleen, which may cause adverse effects. To solve these problems, we adopted convection-enhanced delivery (CED) for drug administration. This technique enables the delivery of boron compounds to the tumor cells in the brain without going through the disrupted BBB. CED, a method for local drug infusion directly into the brain,[10] enables the distribution of any drugs homogeneously in the brain, keeping high concentration at the target site without mechanical damage to the surrounding normal tissue. CED depends on the bulk flow in the interstitial space produced by continuous slow infusion into the brain under low positive pressure. Using this method, it is theoretically possible to deliver drugs to regions where tumor cells invade microscopically with little accumulation in the blood and other organs. Moreover, because it does not depend on the molecular weight of the infused agent, this method allows us to widely select many kinds of therapeutic agents or carriers for them, such as liposomes, dendrimers, and nanotubes.[7,11-15] Today, some clinical trials of targeted toxins with epidermal growth factor receptor, transferrin receptor, interleukin-13 receptor, and interleukin-4 receptor are reported.[8,11,16-18]

In BNCT, there is some interval before neutron irradiation, unlike with chemotherapies or therapies by toxins. This interval derives from the nontoxicity of BDS, and it enables us to estimate the distribution of infusion agents before neutron irradiation. We developed a novel liposomal BDS mechanism that encapsulates BSH and an iodine contrast agent, making it possible to trace the intracerebral distribution of the drug by computed tomography (CT).[19] We evaluated 2 BDSs: PEG liposome encapsulating both BSH and Iomeprol (PEG liposome [BSH, Iomeprol]) and TF-PEG liposome (BSH, Iomeprol) administered by CED in rat brain tumor models.

MATERIALS AND METHODS

Preparation of the Boron Compounds

BSH was purchased from Katchem (Prague, Czech Republic). Iomeprol was used as an iodine contrast agent for CT scanning. Iomeprol (MW777.09, concentration 612.4 mg/mL; Iomeron 300; Eisai, Tokyo, Japan), which is very soluble in water and contains 300 mg/mL organically bound iodine, was used as the imaging tracer. PEG liposome (BSH, Iomeprol) and TF-PEG liposome (BSH, Iomeprol) were prepared by one of the authors (S.K.) as reported previously.[20] Transferrin (1:60 transferrin:phospholipid molar ratio; phospholipid concentration, 0.2 mM) (Wako Pure Chemical Industries, Osaka, Japan) was conjugated to the distal ends of 1,2-dioleoyl-sn-glycero-3-phosphoethanolamine-n-[poly(ethyleneglycol)]-hydroxy succinamide (Nippon Oil and Fats, Tokyo, Japan) in micelles at room temperature for 1 hour with gentle stirring. TF-PEG distearoylphosphatidylethanolamine (DSPE) was transferred to preformed PEG liposomes (64:33:3 dipalmitoylphosphatidylcholine (DPPC):cholesterol:DSPE-PEG molar ratio; size <150 nm) loaded with 300 mM BSH:Iomeprol at a 1:1 volume ratio using the micelle transfer method at a 1:33 TF-PEG-DSPE:liposome molar ratio, at 45°C for 3 hours. Both PEG liposome (BSH, Iomeprol) and TF-PEG liposome (BSH, Iomeprol) were prepared using the protocol described by Wei et al[7] with slight modifications.

To evaluate possible adverse effects of PEG liposome (BSH, Iomeprol) and TF-PEG liposome (BSH, Iomeprol) on normal brain parenchyma, 12 Fischer 344 male rats (200-230 g, F344 NSlc; Japan SLC, Shizuoka, Japan) were given a 20-μg ^{10}B infusion of either BDS (n = 6 per BDS) into the right hemisphere by CED. Body weight was measured just before the CED procedure and on days 7 and 14 after the procedure. Some of the rats that were administered either BDS were euthanized on day 7 after the CED procedure for histological evaluation and were perfused with 4% paraformaldehyde; their brains were then processed for histological examination with hematoxylin and eosin staining.

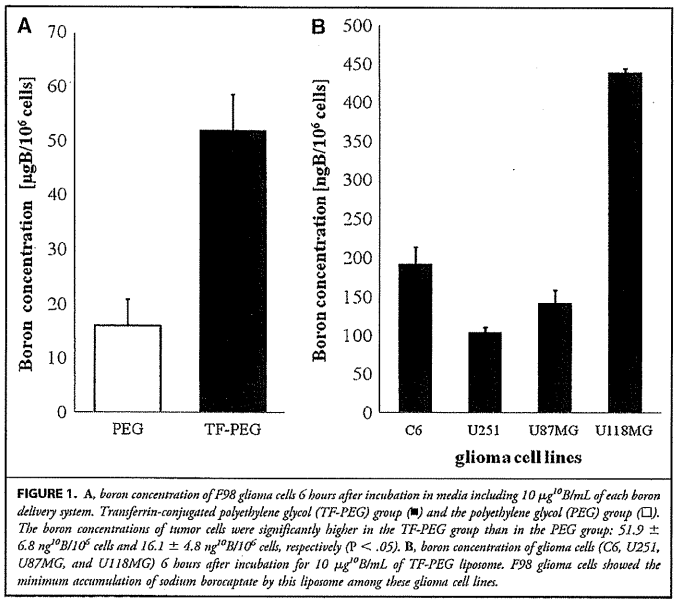

FIGURE 1. **A,** *boron concentration of F98 glioma cells 6 hours after incubation in media including 10 μg^{10}B/mL of each boron delivery system. Transferrin-conjugated polyethylene glycol (TF-PEG) group (■) and the polyethylene glycol (PEG) group (□). The boron concentrations of tumor cells were significantly higher in the TF-PEG group than in the PEG group: 51.9 ± 6.8 ng^{10}B/10^6 cells and 16.1 ± 4.8 ng^{10}B/10^6 cells, respectively (P < .05).* **B,** *boron concentration of glioma cells (C6, U251, U87MG, and U118MG) 6 hours after incubation for 10 μg^{10}B/mL of TF-PEG liposome. F98 glioma cells showed the minimum accumulation of sodium borocuptate by this liposome among these glioma cell lines.*

In Vitro Cellular Uptake Study

For the in vitro boron uptake study, F98 rat glioma cells (provided by Rolf F. Barth MD, The Ohio State University, Columbus, Ohio) were used. One million F98 glioma cells were seeded onto a tissue culture dish (100 × 20 mm; Becton Dickinson, Franklin Lakes, New Jersey) with Dulbecco modified Eagle medium with 10% fetal bovine serum with penicillin and streptomycin at 37°C in an atmosphere of 5% CO_2. All the materials for the culture medium were purchased from Invitrogen (Carlsbad, California). After incubation for 24 hours at 37°C, the medium was replaced with Dulbecco modified Eagle medium containing 10 μg^{10}B/mL PEG liposome (BSH, Iomeprol) or TF-PEG liposome (BSH, Iomeprol), and the cells were incubated for an additional 6 hours at 37°C. The medium was then removed, and the cells were washed twice with phosphate-buffered saline and detached with trypsin–ethylenediamine tetraacetic acid solution. Medium was then added, and the cells were counted and sedimented. Cells were digested overnight with 1 N nitric acid solution (Wako Pure Chemical Industries), and boron uptake was determined by inductively coupled plasma-atomic emission spectrometry (Hitachi, Tokyo, Japan). Cellular uptake of boron by TF-PEG liposome (BSH, Iomeprol) for other glioma cell lines (C6, U251, U87MG, and U118MG) was also evaluated.

Tumor Model

The male Fischer 344 rats were generally anesthetized with an intraperitoneal injection of pentobarbital sodium (50 mg/kg) and placed in a stereotactic frame (Model 900; David Kopf Instruments, Tujunga, California). A midline incision was made in the scalp, and the skull target (3.5 mm right to the bregma) was identified. A hand-held drill was used to create a small burr hole at this location. A 25 μL Hamilton infusion syringe (model 1700 RN, Hamilton Bonaduz AG, Bonaduz, Switzerland) was fixed on the clamping device of the stereotactic frame. A 26-gauge needle attached to a microsyringe was first inserted to a depth of 6.0 mm from the skull and then withdrawn to its target depth in the brain (5.5 mm from the skull surface). Ten thousand F98 cells diluted in 10 μL of Dulbecco modified Eagle medium were then injected over approximately 10 minutes. The needle was kept in place for 1 minute after infusion and withdrawn slowly. The skull hole was sealed with bone wax, and the scalp was sutured. Under these conditions, the procedure results in tumor growth in all rats, with a median survival time of 23 days.

In Vivo Biodistribution Study

For biodistribution study, 10 days after tumor implantation, rats bearing F98 brain tumors were generally anesthetized and placed in a stereotactic frame as described above. They were administered either PEG liposome (BSH, Iomeprol) or TF-PEG liposome (BSH, Iomeprol) by CED with an infusion syringe pump over 30 minutes at a rate of 0.33 μL/min. The total amount of ^{10}B administered to each rat was 20 μg. We then assayed the ^{10}B concentration of tumor, blood, and normal brain by inductively coupled plasma-atomic emission spectrometry. In this study, we sampled normal tissues from both

TABLE 1. Boron Concentrations in Brain Tumors in Rats Bearing F98 Gliomas to Which Polyethylene Glycol Liposome (Sodium Borocaptate, Iomeprol) or Transferrin-Conjugated Polyethylene Glycol Liposome (Sodium Borocaptate), Iomeprol) Was Administered by Convection-Enhanced Delivery[a]

		Boron Concentration, μg/g				Tumor Brain Ratio	
BDS	Time, h[b]	Tumor	Brain Ipsilateral	Brain Contralateral	Blood	Ipsilateral Normal Brain	Contralateral Normal Brain
PEG liposome (BSH, Iomeprol)	0[c]	33.5 ± 10.5	0.6 ± 0.6	0.3 ± 0.1	0.4 ± 0.2	55.8	111.7
	24	22.5 ± 6.1	1.7 ± 1.5	1.0 ± 0.6	0.4 ± 0.1	13.2	22.5
	48	8.5 ± 7.9	1.5 ± 0.7	0.4 ± 0.3	0.4 ± 0.1	5.7	21.3
	72	4.9 ± 4.6	0.2 ± 0.1	0.2 ± 0.1	0.5 ± 0.2	24.5	24.5
TF-PEG liposome (BSH, Iomeprol)	0[c]	55.2 ± 26.6	2.1 ± 2.5	0.4 ± 0.2	0.6 ± 0.3	26.3	138.0
	24	82.2 ± 18.6	0.7 ± 0.4	0.3 ± 0.2	0.6 ± 0.1	117.0	274.0
	48	41.2 ± 14.4	1.2 ± 1.0	0.9 ± 0.6	0.9 ± 0.1	34.3	45.8
	72	25.8 ± 13.5	0.4 ± 0.2	0.4 ± 0.2	0.6 ± 0.2	64.5	64.5

[a]Each point represents the mean ± standard deviation. BDS, boron delivery system; PEG, polyethylene glycol; BSH, sodium borocaptate; TF-PEG, transferrin-conjugated polyethylene glycol.
[b]Hours after convection-enhanced delivery of each BDS.
[c]The time point of 0 means the point just after rats were killed.

hemispheres and defined the normal tissue from the tumor-bearing hemisphere as ipsilateral normal brain and the normal tissue from the other hemisphere as contralateral normal brain. The normal brain of the ipsilateral side, at least a couple of millimeters away from the tumor border, was sampled with approximately 1 g for ^{10}B content measurement. The normal brain of the contralateral side, symmetrical for the ipsilateral sampling, was sampled for the measurement.

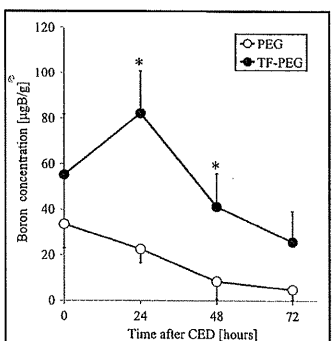

FIGURE 2. *Boron concentration of the tumor at selected times after convection-enhanced delivery (CED) administration of each boron delivery system, polyethylene glycol (PEG) liposome (sodium borocaptate [BSH], Iomeprol) or transferrin-conjugated polyethylene glycol (TF-PEG) liposome (BSH, Iomeprol). The TF-PEG group (●) and the PEG group (○). At all the time points, the tumor boron concentration in the TF-PEG group was higher than that in the PEG group. Especially at 24 and 48 hours after CED, the boron concentrations in the TF-PEG group were significantly higher than those in the PEG group ($P < .05$).*

Imaging Study

For the imaging study, at selected times (0, 24, 48, and 72 hours) after termination of CED, rats were analyzed by CT to evaluate the distribution of BDS and were then euthanized. In this study, we used a high-speed helical CT imaging system (Aquilion 64; Toshiba Medical Systems, Tochigi, Japan). Real-time coronal CT scans (1-mm slice thickness, 1-mm spacing) were performed. We also did a covisualization study using iodine contrast agent (Iomeprol) and fluorescence dye, co-encapsulated into the TF-PEG liposome infused by CED with the CT scan the same as for BDS.

All procedures were performed according to the Osaka Medical College Regulations on Animal Experimentation.

Statistical Analysis

Pairwise comparisons were conducted using Student's t test. Group differences resulting in P values of <.05 were considered statistically significant.

RESULTS

Evaluation of the Normal Rat Brain Infused BDS by CED

Fischer 344 rats receiving a 20-μg ^{10}B infusion of PEG liposome (BSH, Iomeprol) or TF-PEG liposome (BSH, Iomeprol) by CED into their right hemisphere showed no substantial evidence of adverse effects over a 14-day period. Daily observations revealed no clinical deficits during the study. The rats appeared healthy and gained or maintained body weight at the same rate as did normal rats. Histological evaluation from a representative rat euthanized on day 7 after infusion revealed some evidence of tissue inflammation in the striatal regions proximal to the needle track on the site. This tissue reaction was observed only adjacent to the needle tract (data not shown).

In Vitro Uptake Study

The boron concentrations of F98 glioma cells 6 hours after exposure to TF-PEG liposome (BSH, Iomeprol) were significantly higher than those after exposure to PEG liposome (BSH, Iomeprol): 51.9 ± 6.8 and 16.1 ± 4.8 ng$^{10}B/10^6$ cells, respectively. (Figure 1) ($P < .05$).

F98 glioma line showed the minimum accumulation of BSH by TF-PEG liposomes among other glioma lines (C6, U251, U87MG, and U118MG).

In Vivo Biodistribution Study

Table 1 summarizes the biodistribution data for PEG liposome (BSH, Iomeprol) and TF-PEG liposome (BSH, Iomeprol) after CED administration to rats bearing F98 brain tumors. The boron concentrations in tumors were significantly higher in the TF-PEG group than in the PEG group at 24 and 48 hours after CED (Figure 2) ($P < .05$). Especially at 24 hours after CED, the TF-PEG group showed a higher mean tumor boron concentration (82.2 ± 18.6 μg^{10}B/g) and a higher tumor-to-normal brain ratio (274). On the other hand, at that time point, the boron concentrations of blood and contralateral normal brain were less than 1.0 μg^{10}B/g. In addition, the boron concentrations in the other organs such as liver, spleen, kidney, heart, lung, muscle, and skin were also less than 1.0 μg^{10}B/g (data not shown).

Imaging Study

Figures 3 and 4 show the results of the imaging study by CT and histological study of the brain from same rats, respectively, at 4 time points (0, 24, 48, and 72 hours). The CT images showed that the contrast enhancement of the tumor in the TF-PEG group was retained for at least until 72 hours after CED, whereas in the PEG group, the enhancement had already disappeared by 24 hours after CED. The mean Hounsfield unit values in the PEG group and the TF-PEG group were 269 ± 33.3 and 281 ± 88.4, respectively, at 0 hours, and 142 ± 40.6 and 256 ± 39.2, respectively, at 24 hours ($P < .05$) (Figure 5).

In the covisualization study using iodine contrast agent (Iomeprol) and fluorescence dye, co-encapsulated into the TF-PEG liposome administered by CED shows compatible distribution of both agents (left, fluorescencephotography; right, CT scan) (see Figure, Supplemental Digital Content 1, http://links.lww.com/NEU/A371).

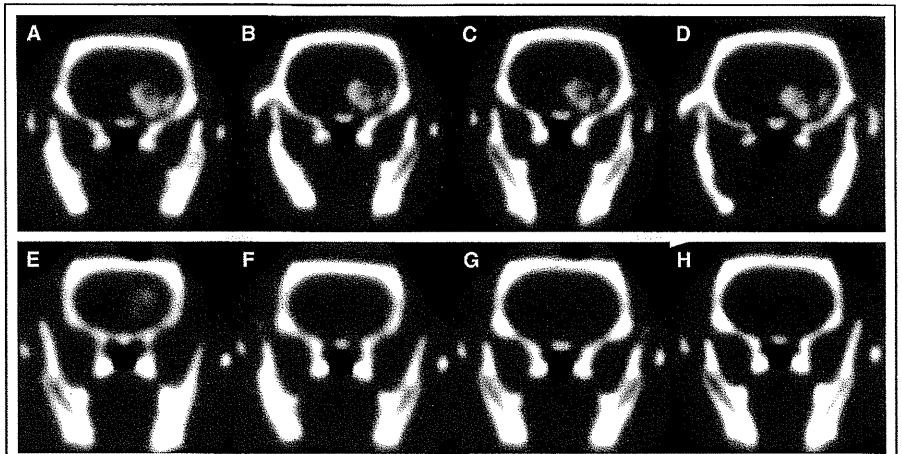

FIGURE 3. *Computed tomography (CT) imaging of iodine contrast agent distributions from each boron delivery system (BDS). These are images from CT scans at selected times (0, 24, 48, 72 hours) after the termination of convection-enhanced delivery (CED) with each BDS. The upper column (A-D) shows one of the polyethylene glycol (PEG) group, and the lower (E-H) shows one of the transferrin-conjugated polyethylene glycol (TF-PEG) group (E-H) The images are from the TF-PEG group, and the contrast enhancement was retained in the tumor until 72 hours after CED. (A-D) The images are from the PEG group. The contrast enhancement had already disappeared 24 hours after CED.*

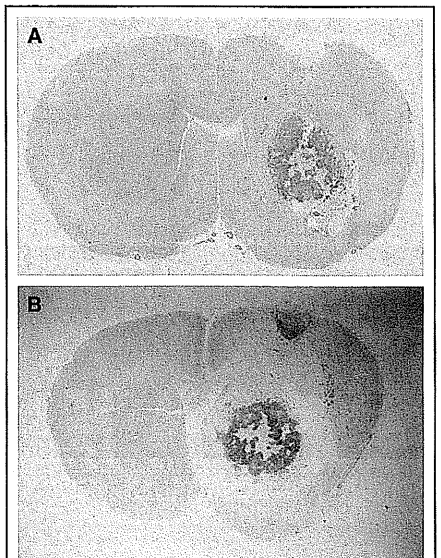

FIGURE 4. *Histological study of the brain shown in Figure 3.* **A** *is from the TF-PEG group and* **B** *is from the polyethylene glycol (PEG) group. Each case shows that the tumor location on hematoxylin and eosin staining corresponds to the tumor contrast on computed tomography imaging in Figure 3.*

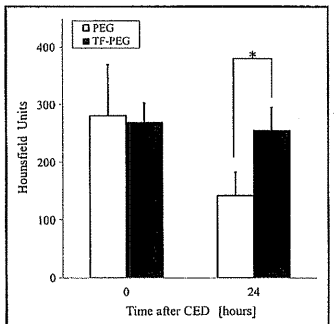

FIGURE 5. *The Hounsfield unit graph measured on each computed tomography image shown in Figure 3. Transferrin-conjugated polyethylene glycol (TF-PEG) group (□) and the polyethylene glycol (PEG) group (■). In both cases, the Hounsfield units at 0 hours after convection-enhanced delivery (CED) are almost the same. In the TF-PEG group, the Hounsfield units remained high until 24 hours after CED, but in the PEG group, the Hounsfield units decreased until 24 hours after CED.*

DISCUSSION

We previously reported that significantly higher concentrations of ^{10}B in tumor tissues in U87Δ brain tumor-bearing nude mice were achieved with systemic TF-PEG liposome (BSH) administration compared with mice administered PEG liposome (BSH) or bare BSH.[9] However, the results of that study led us to speculate on 2 problems: the limitation on ^{10}B accumulation because of the BBB, especially in the microscopic tumor cell invasion area, and the unexpected accumulation into other organs. In this study, to overcome these problems, we devised a combination of tumor targeting by transferrin and CED as a method for local drug injection directly into the brain independent of the BBB. Moreover, we devised a novel liposomal BDS that contained Iomeprol as an iodine contrast agent simultaneously with BSH to visualize the distribution of these BDSs in the brain by using CT.

The results of this in vitro boron uptake study confirmed that TF-PEG liposome can deliver BSH into F98 cells efficiently. As for the in vivo biodistribution study, we found that TF-PEG liposome can also accumulate ^{10}B at significantly high concentrations in the tumor tissue by CED, whereas low ^{10}B concentrations are maintained in normal brain, blood, and other organs. Neutron irradiation is expected to provide immeasurable tumor control efficacy by virtue of this enormously higher contrast in ^{10}B concentration to the normal brain, allowing decreased irradiation doses to the surrounding normal tissues. F98 glioma cell line showed the minimum accumulation of BSH by TF-PEG liposomes among 5 glioma cell lines tested in this study. Therefore, if we use other cell lines in vivo study, more promising results may be expected.

CED itself is a less invasive procedure, and Lonser et al[21] reported that histological inflammation was typical only within a 50-μm radius of the catheter if the agent infused was nontoxic. They also reported that CED had been proved safe in a number of species, ranging from mice to humans, and did not produce cerebral edema or measurably increased intracranial pressure. On the other hand, Saito et al[13] reported that a heterogeneous tissue arrangement of the tumor gives rise to an irregular distribution of the infused agent and to leakage into undesirable areas. They also mentioned that ideal and expected tissue distribution after CED can be significantly decreased when the catheter tip is placed near a large blood vessel, white matter tracts, or the resection cavity because of fluid escaping along the path of least resistance.

Thus, the idea of using imaging to visualize locally injected agents would logically arise. We devised a novel liposomal BDS containing Iomeprol, an iodine contrast agent, simultaneously

with BSH. Using imaging technology, such as CT, this liposomal BDS was successfully visualized and its distribution was well recognized on CT imaging even when injected into the small brain of the rat by CED.

In BNCT, unlike other therapies with cytotoxic agents such as targeted toxins[22] or anticancer drugs, the infused agent itself has no cytotoxicity until neutron irradiation is applied. So if some technical errors, such as those that Saito et al mentioned, in CED were revealed on a CT image (eg, an undesirable distribution of BDS that leaked into the cerebral ventricle or subarachnoid space), neutron irradiation could be postponed so that the safety of the therapy would be ensured. Rousseau et al[19] reported the efficacy of an iodine tracer not only as a tumor contrast agent on CT imaging but also as a dose-enhancement agent for synchrotron stereotactic radiotherapy. Their method also required precise tumor targeting, so they should have encountered the same problems as those in our study with regard to BNCT. They also adopted CED to improve iodine distribution for synchrotron stereotactic radiotherapy treatment and mentioned that its efficacy and safety in that CED can achieve high iodine concentrations in the target area and low iodine concentrations in the surrounding healthy brain tissues and blood vessels. With or without cytotoxicity of the infused agent, visualization through clinical imaging is essential for the treatment of malignant brain tumors.

In the current study, some problems arose. First, it has not been solved how the infused BDSs, liposomes, and encapsulated BSH and Iomeprol were metabolized. In Figures 2 and 4, ^{10}B concentration in tumor tissue is not proportional to Hounsfield unit value at the concerned time. This shows that there is a difference in behavior after injection between BSH and Iomeprol. If the metabolic kinetics of the BDS were disclosed, it would enable us to evaluate the ^{10}B concentration in tumor tissue by CT and Hounsfield unit value. We overcame one of the important problems of CED that caused undesirable distribution of the BDS, such as leaking into the cerebral ventricle or subarachnoid space, by co-encapsulation with drug and contrast agent for CT imaging. However, distribution of the BDS was accurately tracked by the CT imaging. Second, we could not apply neutron irradiation to evaluate the true toxicity and the therapeutic efficacy of this BDS in the current study because both reactors (KUR and JRR4) in Japan had been unavailable because of repairs and the change to uranium as fuel.

In the next step of our work, we expect to confirm that our novel strategy can obtain higher efficacy in BNCT.

Disclosure

This work was supported by Grants-in-Aid for Scientific Research for Young Scientists (B) (18791030 to S.K. and 20791022 to N.I.), by Grants-in-Aid for Scientific Research (C) (20591728 to S.K.) and (B) (19390385 to S-I.M.) from the Japanese Ministry of Education, Culture, Sports, Science and Technology, and by the Eisai Science Foundation to S.K. This work was also supported in part by the Takeda Science Foundation for Osaka Medical College. The authors have no personal financial or institutional interest in any of the drugs, materials, or devices described in this article.

REFERENCES

1. Miyatake S, Kawabata S, Nonoguchi N, et al. Pseudoprogression in boron neutron capture therapy for malignant gliomas and meningiomas. *Neuro Oncol.* 2009;11(4):430-436.
2. Miyatake S, Kawabata S, Yokoyama K, et al. Survival benefit of Boron neutron capture therapy for recurrent malignant gliomas. *J Neurooncol.* 2009;91(2):199-206.
3. Miyatake S, Kawabata S, Kajimoto Y, et al. Modified boron neutron capture therapy for malignant gliomas performed using epithermal neutron and two boron compounds with different accumulation mechanisms: an efficacy study based on findings on neuroimages. *J Neurosurg.* 2005;103(6):1000-1009.
4. Kawabata S, Miyatake S, Kajimoto Y, et al. The early successful treatment of glioblastoma patients with modified boron neutron capture therapy. Report of two cases. *J Neurooncol.* 2003;65(2):159-165.
5. Kawabata S, Miyatake S, Kuroiwa T, et al. Boron neutron capture therapy for newly diagnosed glioblastoma. *J Radiat Res (Tokyo).* 2009;50(1):51-60.
6. Barth RF, Coderre JA, Vicente MG, Blue TE. Boron neutron capture therapy of cancer: current status and future prospects. *Clin Cancer Res.* 2005;11(11):3987-4002.
7. Wei Q, Kullberg EB, Gedda L. Trastuzumab-conjugated boron-containing liposomes for tumor-cell targeting: development and cellular studies. *Int J Oncol.* 2003;23(4):1159-1165.
8. Yang W, Barth RF, Adams DM, et al. Convection-enhanced delivery of boronated epidermal growth factor for molecular targeting of EGF receptor-positive gliomas. *Cancer Res.* 2002;62(22):6552-6558.
9. Doi A, Kawabata S, Iida K, et al. Tumor-specific targeting of sodium borocaptate (BSH) to malignant glioma by transferrin-PEG liposomes: a modality for boron neutron capture therapy. *J Neurooncol.* 2008;87(3):287-294.
10. Bobo RH, Laske DW, Akbasak A, Morrison PF, Dedrick RL, Oldfield EH. Convection-enhanced delivery of macromolecules in the brain. *Proc Natl Acad Sci U S A.* 1994;91(6):2076-2080.
11. Wu G, Barth RF, Yang W, Kawabata S, Zhang L, Green-Church K. Targeted delivery of methotrexate to epidermal growth factor receptor-positive brain tumors by means of cetuximab (IMC-C225) dendrimer bioconjugates. *Mol Cancer Ther.* 2006;5(1):52-59.
12. Mukundan S Jr, Ghaghada KB, Badea CT, et al. A liposomal nanoscale contrast agent for preclinical CT in mice. *AJR Am J Roentgenol.* 2006;186(2):300-307.
13. Saito R, Bringas JR, McKnight TR, et al. Distribution of liposomes into brain and rat brain tumor models by convection-enhanced delivery monitored with magnetic resonance imaging. *Cancer Res.* 2004;64(7):2572-2579.
14. Dickinson PJ, LeCouteur RA, Higgins RJ, et al. Canine model of convection-enhanced delivery of liposomes containing CPT-11 monitored with real-time magnetic resonance imaging: laboratory investigation. *J Neurosurg.* 2008;108(5):989-998.
15. Aoki I, Bakalova R. MR molecular imaging using drug delivery system. *Drug Delivery System.* 2008;23(1):61-68.
16. Weaver M, Laske DW. Transferrin receptor ligand-targeted toxin conjugate (Tf-CRM107) for therapy of malignant gliomas. *J Neurooncol.* 2003;65(1):3-13.
17. Murad GJ, Walbridge S, Morrison PF, et al. Real-time, image-guided, convection-enhanced delivery of interleukin 13 bound to pseudomonas exotoxin. *Clin Cancer Res.* 2006;12(10):3145-3151.
18. Vogelbaum MA. Convection enhanced delivery for the treatment of malignant gliomas: symposium review. *J Neurooncol.* 2005;73(1):57-69.
19. Rousseau J, Boudou C, Esteve F, Elleaume H. Convection-enhanced delivery of an iodine tracer into rat brain for synchrotron stereotactic radiotherapy. *Int J Radiat Oncol Biol Phys.* 2007;68(3):943-951.
20. Maruyama K, Ishida O, Kasaoka S, et al. Intracellular targeting of sodium mercaptoundecahydrododecaborate (BSH) to solid tumors by transferrin-PEG liposomes, for boron neutron-capture therapy (BNCT). *J Control Release.* 2004;98(2):195-207.
21. Lonser RR, Walbridge S, Garmestani K, et al. Successful and safe perfusion of the primate brainstem: in vivo magnetic resonance imaging of macromolecular distribution during infusion. *J Neurosurg.* 2002;97(4):905-913.
22. Rainov NG, Soling A. Clinical studies with targeted toxins in malignant glioma. *Rev Recent Clin Trials.* 2006;1(2):119-131.

***Supplemental digital content** is available for this article. Direct URL citations appear in the printed text and are provided in the HTML and PDF versions of this article on the journal's Web site (www.neurosurgery-online.com).*

Acknowledgments

We thank Dr Rolf F. Barth, Department of Pathology, The Ohio State University, for preparing the F98 cell line and Hitomi Kuroda for technical assistance.

COMMENTS

The authors report a novel means to introduce potential sensitizing agents into an experimental brain tumor in an animal model using convection-enhanced delivery. The goal is to introduce these potential agents into the brain surrounding a tumor mass and eventually administer neutron radiation with the hope of providing greater cell kill, especially in the infiltrated zone. In essence, this is a study showing that specially tailored pharmaceuticals can be created to increase delivery of a selected agent in the target zone and that addition of other agents may make recognition of the target by imaging possible as well. It would be even better to demonstrate in a part 2 study that this targeting of sensitizing compounds actually resulted in a therapeutic response using boron neutron capture therapy (BCNT). This technology has been advocated in a relatively few centers for more than 40 years; perhaps because of the large overhead cost and lack of major therapeutic safety window, it has never reached mainstream use. Further efforts may allow safer BNCT, especially because the authors show that tissue concentrations are significantly reduced in other tissues, an important feature that may improve the safety of BNCT during the actual radiation administration. The risk-benefit ratio in BNCT has been difficult to ascertain. In the past, neutron radiation was effective at killing the target tumor but usually resulted in unacceptable radiation toxicity in the brain. Perhaps further efforts in this field will yet allow a beneficial therapeutic window to emerge.

L. D. Lunsford
Pittsburgh, Pennsylvania

The authors describe their early preclinical findings (in vitro and in vivo) in a potentially interesting application and modification of BCNT. Their strategy directly targets glioma cells (and the surrounding region) with transferrin bound to a polyethylene glycol liposome that encapsulates sodium borocaptate and an iodine contrast agent (used for tracking the liposome distribution during computed tomography imaging). To provide high concentrations of this compound to regions in and around glioma, it was delivered to tumor and surrounding region via convection-enhanced delivery.

The data from this study indicate that the polyethylene glycol liposome encapsulated sodium borocaptate can be safely and successfully delivered by convection-enhanced delivery in rodent brain tumor models while tracking its distribution using computed tomography imaging. Although these early findings are encouraging from a distribution perspective, the next potential step in determining whether this modification of BCNT for glioma may hold promise will be in determining therapeutic dosing (irradiation) and assessing efficacy in vivo. I look forward to the authors' subsequent work in this area.

Russell R. Lonser
Bethesda, Maryland

J Neurooncol (2011) 102:471–475
DOI 10.1007/s11060-010-0333-3

CASE REPORT

Repeated treatments with bevacizumab for recurrent radiation necrosis in patients with malignant brain tumors: a report of 2 cases

Motomasa Furuse · Shinji Kawabata · Toshihiko Kuroiwa · Shin-Ichi Miyatake

Received: 26 April 2010 / Accepted: 23 July 2010 / Published online: 7 August 2010

Abstract Bevacizumab is expected to constitute a new treatment modality for radiation necrosis. In the present cases, we observed a recurrence of radiation necrosis after temporary improvement by bevacizumab treatment. Re-treatment with bevacizumab controlled the necrosis again. A 39-year-old male and a 57-year-old female were diagnosed with glioblastoma and lung cancer metastasis, respectively. The former patient underwent partial resection of the glioblastoma, followed by boron neutron capture therapy (BNCT) and 30 Gy of fractionated X-ray radiotherapy. Eleven months after BNCT, he suffered from left hemiparesis and convulsions with enlargement of a perifocal edema. The latter patient underwent stereotactic radiosurgery twice for the same tumor. Three months after the second radiosurgery, she had an uncontrollable convulsion and right hemiplegia with a massive perifocal edema. Both lesions were suggested to be radiation necroses by positron emission tomography using amino acids as a tracer. Neither patient responded to corticosteroids, anticoagulants, or vitamin E. They underwent treatment with 5 mg/kg bevacizumab biweekly, for a total of 6 cycles. The size of the perifocal edema was clearly reduced in response to the treatments. The neurological status of the patients improved concomitant with therapy. However, the clinical status of both patients was aggravated several months after the bevacizumab was stopped, and the perifocal edemas enlarged again. The patients underwent a second treatment with bevacizumab, and the perifocal edemas again decreased. Although radiation necrosis may recur several months after bevacizumab treatment, repeated bevacizumab treatments also appear to be effective.

Keywords Bevacizumab · Boron neutron capture therapy · Brain edema · Glioblastoma, metastatic brain tumor · Radiation necrosis

Bevacizumab is a humanized murine monoclonal antibody against the vascular endothelial growth factor (VEGF) ligand that has been approved by the FDA in the U.S. to treat colorectal cancer, non-small cell lung cancer, renal cancer, breast cancer, and glioblastoma multiforme [1–5]. In addition, preliminary studies reported that bevacizumab was effective for treating radiation necrosis in the central nervous system [6, 7]. These studies led to a randomized controlled trial that demonstrated class I evidence of the efficacy of bevacizumab treatment for progressive radiation necrosis [8]. In the present work, we report our use of bevacizumab to treat two patients who showed signs of radiation necrosis after radiotherapy for a metastatic brain tumor and a glioblastoma, respectively. In both cases, rapid improvement was achieved both clinically and neuroradiologically after the initial treatment, but the patients worsened several months after the bevacizumab treatment was stopped, and thus a second round of bevacizumab therapy was used. We report the results of these two cases.

Case 1

A 39-year-old male had a right parietal cystic glioblastoma. Fluoride-labeled boronophenylalanine (BPA)-positron emission tomography (PET) was applied for the residual lesion, and the lesion/normal tissue (L/N) ratio was 3.0

M. Furuse · S. Kawabata · T. Kuroiwa · S.-I. Miyatake (✉)
Department of Neurosurgery, Osaka Medical College, 2-7, Daigakumachi, Takatsuki, Osaka 569-8686, Japan
e-mail: neu070@poh.osaka-med.ac.jp

(Fig. 1a). This L/N ratio was representative of glioblastoma [9]. An L/N ratio of greater than 2.5 is strongly suggestive of tumor progression in newly-diagnosed or recurrent glioblastomas, while an L/N ratio of less than 2.0 suggests a high possibility of radiation necrosis or pseudoprogression [9, 10]. Tumor-selective particle radiation, boron neutron capture therapy (BNCT) were applied with a minimum tumor dose of 42.3 Gy-Eq and a maximum brain dose of 11.9 Gy-Eq [10, 11]. Here, Gy-Eq (gray-equivalent) corresponds to an X-ray dose that can yield effects equivalent to total BNCT radiation [10]. This treatment was followed by 30 Gy fractionated X-ray treatment, according to our recent protocol [12], and temozolomide as adjuvant chemotherapy. The residual tumor was decreased in size in follow-up magnetic resonance (MR) images.

Eleven months after BNCT, left hemiparesis and convulsions recurred and the MR images showed re-enlargement of the gadolinium-enhanced lesion with perifocal edema (Fig. 2a, b). BPA-PET was re-applied to determine whether the lesion represented a radiation necrosis or local tumor progression. The L/N ratio in this PET was 1.9, which suggested that the lesion was indeed radiation necrosis (Fig. 1b) [9]. Corticosteroids, anticoagulants, and vitamin E were all tried and were not effective.

The patient underwent treatment with bevacizumab of 5 mg/kg biweekly for 6 cycles in total. MR images revealed that the perilesional edema and gadolinium-enhanced lesion were reduced in size, as shown in Fig. 2c,d. The convulsions were controlled with anticonvulsants, and the hemiparesis improved without use of glucocorticoids.

The patient was restarted on treatment with anticoagulants and vitamin E. Six months later, however, his neurological status was aggravated and MR images demonstrated abnormal enhancement and progression of the perifocal edema (Fig. 3a, b). BPA-PET yielded an L/N ratio of 2.1, suggesting the recurrence of radiation necrosis (Fig. 1c). The L/N ratios in Fig. 2b and c were almost the same (1.9 and 2.1), and compatible with radiation necrosis. He was again treated with 5 mg/kg of bevacizumab every other week. After 3 cycles of bevacizumab, MR images again demonstrated a decrease in the perifocal edema and post-gadolinium enhancement (Fig. 3c, d), and the treatment was stopped. At the time of this writing, the patient has been doing well for more than 4 months without worsening of clinical symptoms.

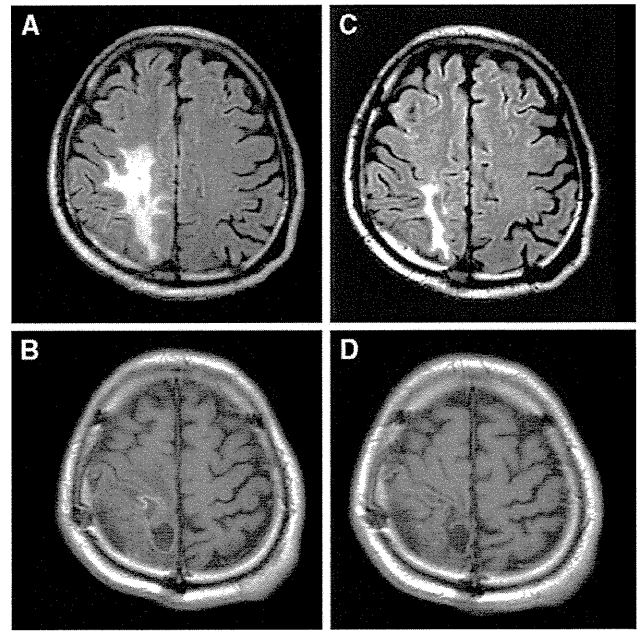

Fig. 2 FLAIR MR images before treatment of bevacizumab (**a**), and after 6 cycles of bevacizumab 5 mg/kg (**c**). Postcontrast T1-weighted MR images before treatment with bevacizumab (**b**), and after 6 cycles of bevacizumab 5 mg/kg (**d**). *Upper row* an extended hyperintense area obviously reduced after bevacizumab treatment. *Lower row* a postcontrast enhanced lesion indistinct after bevacizumab treatment

Case 2

A 57-year-old female experienced a seizure and was diagnosed with a brain metastasis in the left motor strip, which was derived from lung cancer. She underwent repetitive stereotactic radiosurgery (SRS) with a total marginal dose of 49 Gy over a 6-month interval. Three months after the second SRS, her seizures became uncontrollable and right hemiplegia occurred. MR images revealed a progression of perifocal edema and an enhanced lesion (Fig. 4a, b).

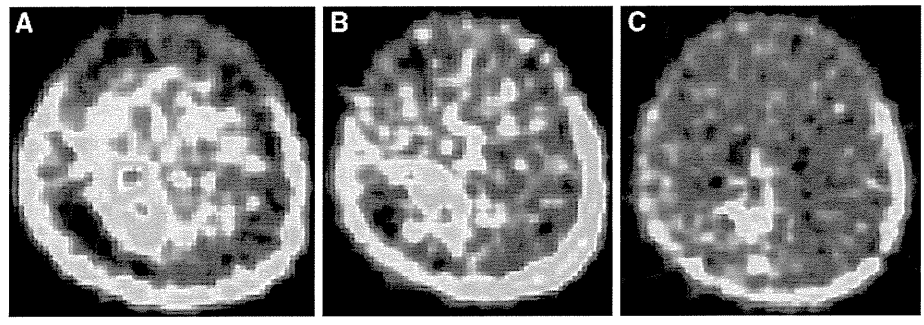

Fig. 1 Serial BPA-PET study in Case 1. **a**: BPA-PET just prior to BNCT (L/N ratio: 3.0). **b**: BPA-PET taken at the first aggravation of clinical symptoms and neuroimages (L/N ratio: 1.9). **c**: BPA-PET taken at the 2nd aggravation (L/N ratio: 2.1)

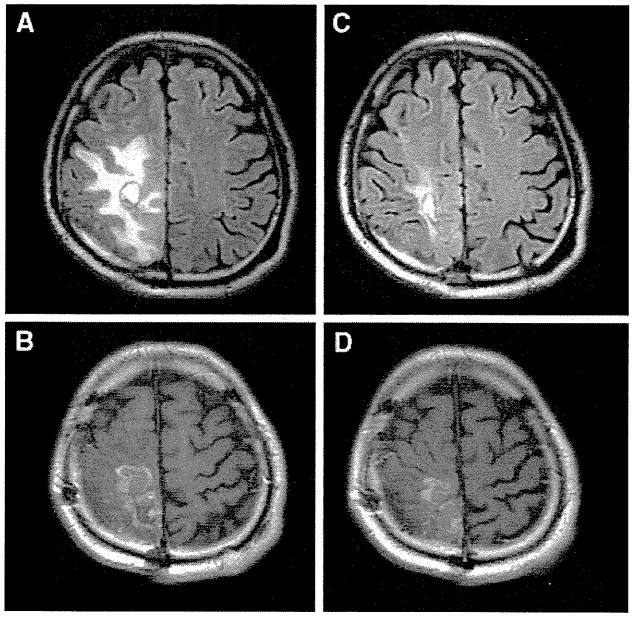

Fig. 3 FLAIR MR images before the second treatment with bevacizumab (**a**) and after 3 cycles of bevacizumab 5 mg/kg (**c**). Postcontrast T1-weighted MR images before the second treatment with bevacizumab (**b**) and after 3 cycles of bevacizumab 5 mg/kg (**d**). *Upper row* an enlarged hyperintense area apparently decreased after the second bevacizumab treatment. *Lower row* postcontrast enhancement became vague after the second bevacizumab treatment

BPA-PET showed a low uptake of BPA, and an L/N ratio of 1.8. Together with the MR findings, these results suggested that the lesion was a radiation necrosis. Her clinical symptoms did not respond to increasing doses of steroids or other medical treatments.

She was treated with 5 mg/kg of bevacizumab every other week. MR images obtained 1 week after one dose showed a dramatic reduction in the hyperintense area on fluid-attenuated inversion recovery (FLAIR) images and attenuation of the abnormal enhanced area on gadolinium-enhanced T1-weighted images (Fig. 4c, d). Subsequent MR images were obtained 1 week after 6 cycles and demonstrated a further decrease in the FLAIR-hyperintense lesion (Fig. 4e). The patient's hemiparesis consistently improved, and she was able to walk by herself. Her performance status improved from grade 2 to grade 3.

At this time, her treatment was reduced to simply anticoagulants and vitamin E. Three months later, her hemiparesis was aggravated and computed tomographic imaging revealed an enlarged low-density area (Fig. 5a). She underwent a second bevacizumab treatment. After 2 cycles of bevacizumab, the MR images showed a decrease in perifocal edema (Fig. 5b), but new multiple metastatic lesions. The bevacizumab treatment was therefore discontinued.

Discussion

Recently, new radiation therapies, such as BNCT, SRS, proton beam radiation, and intensity-modulated radiation therapy, have been performed for patients with malignant gliomas. These high-dose radiation therapeutics have been improving patient survival [11–14], but radiation necrosis in the brain has become a more serious problem. Current treatments for radiation necrosis of the brain include the

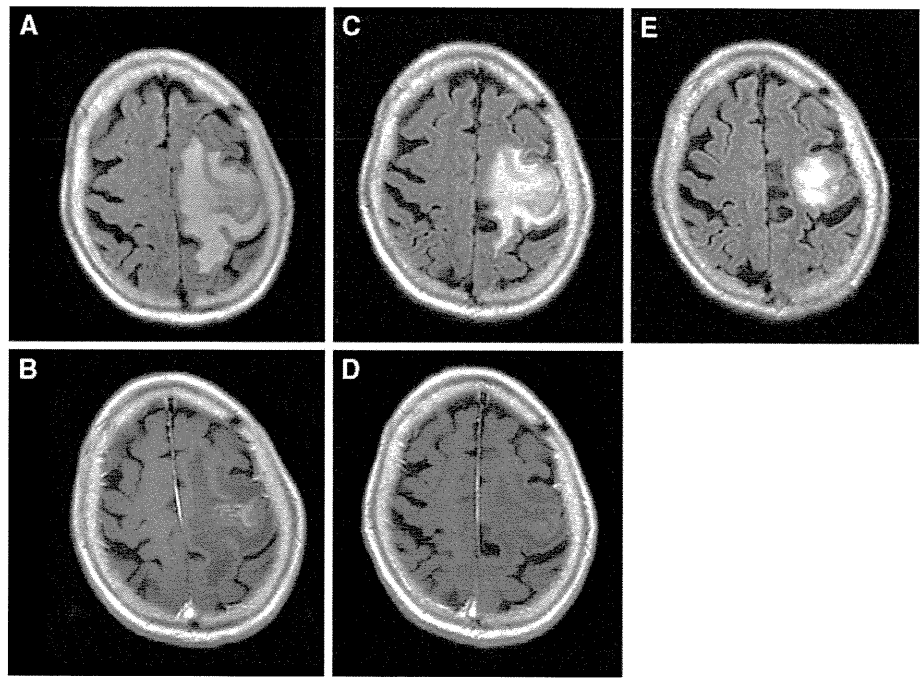

Fig. 4 FLAIR MR images before treatment with bevacizumab (**a**), 1 week after one dose of bevacizumab 5 mg/kg (**c**), and after 6 cycles (**e**). Postcontrast T1-weighted MR images before treatment with bevacizumab (**b**) and 1 week after one dose of bevacizumab 5 mg/kg (**d**). *Upper row* a hyperintense area progressively and dramatically reduced after administration of bevacizumab. *Lower row* a postcontrast enhancement obscured after bevacizumab treatment

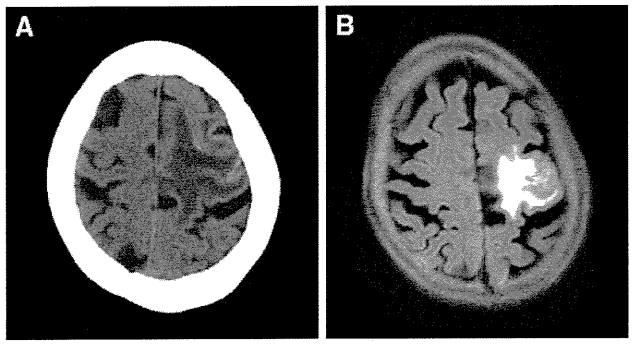

Fig. 5 A computed tomographic image 3 months after the first bevacizumab treatment (**a**) and a FLAIR MR image after 2 cycles of the second bevacizumab treatment (**b**). A perilesional edema decreased after the second bevacizumab treatment

use of corticosteroids, anticoagulants, and vitamin E, as well as hyperbaric oxygenation and surgical resection [15–19]. Corticosteroids are often effective in the early phase of radiation injury, but are ineffectual in late radiation injury. Radiation injury includes damage of the vascular endothelial cells, leading to an increase in vascular permeability [20, 21]. Bevacizumab is theoretically effective against radiation injury because VEGF is known as a vascular permeability factor [22]. Gonzalez et al. [6] first reported the effects of bevacizumab on radiation necrosis of brain tumors. They reviewed the cases of 8 patients with recurrent malignant gliomas and radiation necrosis who were treated with bevacizumab, and in some cases with temozolomide or other anticancer agents as well, Radiation necrosis was diagnosed by biopsy in 2 of these patients and by MR images in 6. All 8 patients showed improvement on MR images within 8 weeks of the bevacizumab treatment. Another report by Torcuator et al. [7] also demonstrated the effectiveness of bevacizumab on cerebral radiation necrosis. They confirmed radiation necrosis by biopsy in all 6 patients. Neither of these earlier reports mentioned whether or not radiation necrosis recurred.

In the present case reports, radiation necrosis recurred several months after bevacizumab treatment in both patients. Our patients showed the same initial response to bevacizumab as in the two previous reports. However, in our cases, the bevacizumab treatment did not permanently eradicate the radiation necrosis, and the necrosis recurred. We found bevacizumab effective in treating recurrent radiation necrosis. In the study reported by Levin et al. [8], three patients benefited by retreatment with bevacizumab. In our report, we also found that radiation necrosis can be controlled with bevacizumab treatment as initial treatment as well as in the event of post-bevacizumab recurrence of radiation necrosis.

Our diagnosis of radiation necrosis was based on BPA-PET and serial MR images. Although the findings of BPA-PET were correlated to histopathological results in our previous study [9], BPA-PET is not a proven radiographic modality. Therefore, our patients were presumed to have radiation necrosis, because the histopathological findings of biopsy or surgical resection are considered definitive for a diagnosis of radiation necrosis. Surgical resection is an important modality if brain edema does not respond to medical treatment and the lesions are resectable. In one of the present cases, because the lesion itself involved the motor strip, a lesionectomy was out of the question. Based on the present findings, bevacizumab can be considered a new treatment modality for both new and recurrent radiation necrosis of the brain, especially for unresectable lesions, as shown here. Its use would influence not only the treatment strategy for radiation necrosis, but also radiotherapeutic dose planning for unresectable tumors.

Conclusion

We used bevacizumab in the treatment of two patients with radiation necrosis of brain tumors. Several months later, however, radiation necrosis recurred in both patients. Repeated therapy with bevacizumab was similarly effective against the recurrent radiation necrosis. Moreover, bevacizumab appears to be an effective treatment for radiation necrosis, especially for lesions located in an eloquent area because radiation necrosis in this area is surgically inaccessible.

Acknowledgments This work was partly supported by a Grant-in-Aid for Scientific Research (B) (19390385 to S.I.M.) from the Japanese Ministry of Education, Science and Culture and in part by the Takeda Science Foundation for Osaka Medical College.

References

1. Hurwitz H, Fehrenbacher L, Novotny W, Cartwright T, Hainsworth J, Heim W, Berlin J, Baron A, Griffing S, Holmgren E, Ferrara N, Fyfe G, Rogers B, Ross R, Kabbinavar F (2004) Bevacizumab plus irinotecan, fluorouracil, and leucovorin for metastatic colorectal cancer. N Engl J Med 350:2335–2342
2. Sander A, Gray R, Perry MC, Brahmer J, Schiller JH, Dowlati A, Lilenbaum R, Johnson DH (2006) Paclitaxel-carboplatin alone or with bevacizumab for non-small-cell lung cancer. N Engl J Med 355:2542–2550
3. Escudier B, Pluzanska A, Koralewski P, Ravaud A, Bracarda S, Szczlik C, Chevreau C, Filipek M, Melichar B, Bajetta E, Gorbunova V, Bay JO, Bodrogi I, Jagiello-Gruszfeld A, Moore N, AVOREN Trial Investigators (2007) Bevacizumab plus interferon alfa-2a for treatment of metastatic renal cell carcinoma: a randomized, double-blind phase III trial. Lancet 370:2103–2111
4. Miller KD, Chap LI, Holmes FA, Cobleigh MA, Marcom PK, Fehrenbacher L, Dickler M, Overmoyer BA, Reimann JD, Sing AP, Langmuir V, Rugo HS (2005) Randomized phase III trial of capecitabine compared with bevacizumab plus capecitabine in

patients with previously treated metastatic breast cancer. J Clin Oncol 23:792–799
5. Vredenburgh JJ, Desjardins A, Herndon JE IId, Marcello J, Reardon DA, Quinn JA, Rich JN, Sathornsumetee S, Gururangan S, Sampson J, Wagner M, Bailey L, Bigner DD, Friedman AH, Friedman HS (2007) Bevacizumab plus irinotecan in recurrent glioblastoma multiforme. J Clin Oncol 25:4722–4729
6. Gonzalez J, Kumar AJ, Conrad CA, Levin VA (2007) Effect of bevacizumab on radiation necrosis of the brain. Int J Radiat Oncol Biol Phys 67:323–326
7. Torcuator R, Zuniga R, Mohan YS, Rock J, Doyle T, Anderson J, Gutierrez J, Ryu S, Jain R, Rosenblum M, Mikkelsen T (2009) Initial experience with bevacizumab treatment for biopsy confirmed cerebral radiation necrosis. J Neurooncol 94:63–68
8. Levin VA, Bidaut L, Hou P, Kumar AJ, Wefel JS, Bekele N, Prabhu S, Loghin M, Gilbert MR, Jackson EF (2010) Randomized double-blind placebo-controlled trial of bevacizumab therapy for radiation necrosis of the central nervous system. Int J Radiat Oncol Biol Phys. doi:10.1016/j.ijrobp.2009.12.061
9. Miyashita M, Miyatake S, Imahori Y, Yokoyama K, Kawabata S, Kajimoto Y, Shibata MA, Otsuki Y, Kirihata M, Ono K, Kuroiwa T (2008) Evaluation of fluoride-labeled boronophenylalanine-PET imaging for the study of radiation effects in patients with glioblastomas. J Neurooncol 89:239–246
10. Miyatake S, Kawabata S, Nonoguchi N, Yokoyama K, Kuroiwa T, Matsui H, Ono K (2009) Pseudoprogression in boron neutron capture therapy for malignant gliomas and meningiomas. Neurooncology 11:430–436
11. Miyatake S, Kawabata S, Kajimoto Y, Aoki A, Yokoyama K, Yamada M, Kuroiwa T, Tsuji M, Imahori Y, Kirihata M, Sakurai Y, Masunaga S, Nagata K, Maruhashi A, Ono K (2005) Modified boron neutron capture therapy for malignant gliomas performed using epithermal neutron and two boron compounds with different accumulation mechanisms: an efficacy study based on findings on neuroimages. J Neurosurg 103:1000–1009
12. Kawabata S, Miyatake SI, Kuroiwa T, Yokoyama K, Doi A, Iida K, Miyata S, Nonoguchi N, Michiue H, Takahashi M, Inomata T, Imahori Y, Kirihata M, Sakurai Y, Maruhashi A, Kumada H, Ono K (2009) Boron neutron capture therapy for newly diagnosed glioblastoma. J Radiat Res (Tokyo) 50:51–60
13. Fitzek MM, Thornton AF, Rabinov JD, Lev MH, Pardo FS, Munzenrider JE, Okunieff P, Bussiere M, Braun I, Hochberg FH, Hedley-Whyte ET, Liebsch NJ, Harsh GR IV (1999) Accelerated fractionated proton/photon irradiation to 90 cobalt gray equivalent for glioblastoma multiforme: results of a phase II prospective trial. J Neurosurg 91:251–260
14. Iuchi T, Hatano K, Narita Y, Kodama T, Yamaki T, Osato K (2006) Hypofractionated high-dose irradiation for the treatment of malignant astrocytomas using simultaneous integrated boost technique by IMRT. Int J Radiat Oncol Biol Phys 64:1317–1324
15. Delanian S, Balla-Mekias S, Lefaix JL (1999) Striking regression of chronic radiotherapy damage in a clinical trial of combined pentoxifylline and tocopherol. J Clin Oncol 17:3283–3290
16. Glantz MJ, Burger PC, Friedman AH, Radtke RA, Massey EW, Schold SC Jr (1994) Treatment of radiation-induced nervous system injury with heparin and warfarin. Neurology 44:2020–2027
17. Rizzoli HV, Pagnanelli DM (1984) Treatment of delayed radiation necrosis of the brain. A clinical observation. J Neurosurg 60:589–594
18. Shaw PJ, Bates D (1984) Conservative treatment of delayed cerebral radiation necrosis. J Neurol Neurosurg Psychiatry 47: 1338–1341
19. Tandon N, Vollmer DG, New PZ, Hevezi JM, Herman T, Kagan-Hallet K, West GA (2001) Fulminant radiation-induced necrosis after stereotactic radiation therapy to the posterior fossa. Case report and review of the literature. J Neurosurg 95:507–512
20. Coderre JA, Morris GM, Micca PL, Hopewell JW, Verhagen I, Kleiboer BJ, van der Kogel AJ (2006) Late effects of radiation on the central nervous system: role of vascular endothelial damage and glial stem cell survival. Radiat Res 166:495–503
21. Kimura T, Sako K, Tohyama Y, Aizawa S, Yoshida H, Aburano T, Tanaka K, Tanaka T (2003) Diagnosis and treatment of progressive space-occupying radiation necrosis following stereotactic radiosurgery for brain metastasis: value of proton magnetic resonance spectroscopy. Acta Neurochir (Wien) 145:557–564
22. Midgley R, Kerr D (2005) Bevacizumab—current status and future directions. Ann Oncol 16:999–1004